HYDROGELS WITH DYNAMIC BIOCHEMICAL ENVIRONMENTS FOR 3D CELL CULTURE

HYDROGELS WITH DYNAMIC BIOCHEMICAL ENVIRONMENTS FOR 3D CELL CULTURE

By DEVANG NIJSURE, B.Sc.

A Thesis Submitted to the School of Graduate Studies in Fulfilment of the Requirements for the Degree Master of Science

TITLE: HYDROGELS WITH DYNAMIC BIOCHEMICAL ENVIRONMENTS

FOR 3D CELL CULTURE

AUTHOR: DEVANG NIJSURE, B.Sc.

SUPERVISOR: Professor Ryan Wylie, McMaster University

Abstract

The *in vivo* 3D extracellular matrix provides a temporal regulatory environment of chemical cues. Understanding this dynamic environment will be crucial for efficient drug screening, diseases mechanism elucidation, and tissue engineering. Therefore, *in vitro* 3D cell culture systems with reversible chemical environments are required. To this end, we developed a non-cytotoxic agarose-desthiobiotin hydrogel to sequester streptavidin biomolecule conjugates (K_D 10^{-11} M), which can then be displaced by the addition of biotin (K_D 10^{-15} M). Streptavidin biomolecule conjugates were simultaneously and sequentially immobilized by changing media components. The time required for biochemical environment exchange was minimized by increasing the surface area to volume ratios and pore size of the hydrogels. We temporally controlled the cell adhesive properties of hydrogels with RGD modified streptavidin to influence endothelial cell tube formation.

Acknowledgements

I would like to thank Professor Ryan Wylie for his tremendous guidance and ideas during my graduate studies. He was always available and would consistently check in with the research group, offering advice or a helping hand. I would also like to thank all the members of the Wylie group, particularly Vincent Huynh for his assistance with organic synthesis and overall help, Catherine Lambert for her work on functionalizing glass slides with silane and preliminary binding studies, and Muneeb Shoiab for his ideas, help and conversation about the shows that apparently only he and I watch.

I would also like to thank Dr. Harald Stover, for being on my committee, and for his insight and advice throughout the course of my graduate project.

I am very grateful to Markus Rose from the Moran-Mirabal research group, for his help and guidance imaging my first batch of porous hydrogels using the Moran-Mirabal groups confocal microscope.

Table of Contents

LIST OF FIGURES

LIST OF ABBREVIATIONS

2D: Two-dimensional

3D: Three-dimensional

3T3: fibroblast cell line

AgD: agarose desthiobiotin

rBMC: rat bone marrow cells

CDI: carbonyl imidazole

DA: Diels Alder

DG: diglycidyl ether

DRG: Dorsal Root Ganglion

DIBAC: dibenzoazacyclooctyne

ECM: Extracellular Matrix

EDC: 1-ethyl-3-(3-dimethylaminopropyl) carbodiimide

FGF-2: Fibroblast Growth Factor-2

HA: hyaluronic acid

HUVEC: human umbilical vein endothelial cells

IL - interleukin

K_d: Equilibrium dissociation constant

NHS: N-hydroxysuccinimide

MALDI-TOF: matrix assisted laser desorption/ionization-time of flight

MSC: mesenchymal stem cells

MW: molecular weight

MMP: matrix metalloproteinase

OSCC: oral squamous cell carcinoma

RGD: arginylglycylaspartic acid

SA: streptavidin

PBA: phenylboronic acid

PBS: phosphate buffered saline

PEG: polyethylene glycol

POEGMA: poly(oligo(ethylene glycol) methyl ether methacrylate

PVA: poly(vinyl alcohol)

VEGF: Vascular Endothelial Growth Factor

1. Introduction

1.1 3D cell culture

The transition from two-dimensional (2D, e.g. cell culture in petri dishes) to three-dimensional (3D) *in vitro* cell culture is required to better mimic the *in vivo* environment and to develop biomaterials for drug screening efficiency[1], disease mechanism elucidation[2], and tissue engineering.[1,3] Cellular behaviour has been shown to vary significantly between 2D and 3D environments because 3D cultures better represent the chemical and mechanical properties of the natural extracellular matrix (ECM).[4]

Cell morphology, which differs in 2D and 3D cell culture, has been shown to strongly influence stem cell proliferation and differentiation.[5] In 2D, cells stretch and spread on flat surfaces, however, *in vivo*, cells adhere in 3D environments and adopt morphologies with greater circularity. McBeath et al. demonstrated that cell shape influences human mesenchymal stem cell (hMSC) differentiation by controlling cell shape with micro-patterns of adhesive ligands on polydimethylsiloxane (PDMS).[6] The least spread out hMSCs differentiated into adipocytes, whereas highly spread hMSCs differentiated into osteoblasts.[6] Baharvand et al. demonstrated that human embryonic stem cell (hESC) differentiation in 3D collagen gels better mimicked *in vivo* conditions than 2D collagen surfaces.[5] Rat bone marrow cell (rBMC) proliferation has also been shown to be enhanced in 3D alginate tubular environments compared to flat 2D alginate surfaces.[7]

3D environments are also important in the design of ECM cancer models.[8] 3D tumour microenvironments increase the proliferation rate of oral squamous cell carcinoma (OSCC-3) cells compared to 2D cultures.[9] Furthermore, 3D OSCC-3 cultures secreted pro-angiogenesis factors (vascular endothelial growth factors (VEGF) and interleukin-8 (IL-8)), whereas 2D monolayers expressed VEGF and IL-8 in non-natural amounts.[9] Therefore, it is crucial to study cells in 3D environments that closely mimic *in vivo* conditions to better understand cellular activities and efficacy of drugs.

1.2 The ECM's biochemical environment

The ECM is a complex regulatory environment with chemical and mechanical cues.[1,8] The remainder of the introduction will focus on the chemical environment to provide context for the developed temporal chemical patterning system for hydrogels.

The ECM scaffold is composed of proteoglycans (e.g. versican, heparan sulfate and chondroitin sulfate), hyaluronic acid, proteins (e.g. collagens and elastins), fibronectin, and laminin.[10,11] Collagen is a structural protein in the ECM with high tensile strength that contains cell adhesive and proteolytic sites.[12] Fibronectin and laminin are ECM glycoproteins that contain cell binding domains (e.g. RGD) to anchor cells in the ECM.[1,13] Proteoglycans mediate ECM hydration levels, and sequester growth factors that direct cell proliferation, migration, differentiation and renewal.[11,14] Soluble macromolecules (growth factors, chemokines, cytokines and peptides) are sequestered within the ECM and serve as cell signaling molecules.[8,15] The ECM helps

regulate the availability of soluble macromolecules, thus controlling their distribution, activation and presentation.

Many proteins contain heparan binding domains for localization in the ECM.[10] For example, fibroblast growth factors (FGFs) and VEGFs bind to ECM proteoglycans.[10,16] The ECM acts as a reservoir for growth factors and helps establish gradients.[10,17,18] Furthermore, growth factor activity is influenced by the complexation between cell receptors and ECM components. [18,19] Therefore, the chemical environment of the ECM is crucial for cellular activity and methods are being developed to mimic the natural chemical environment.
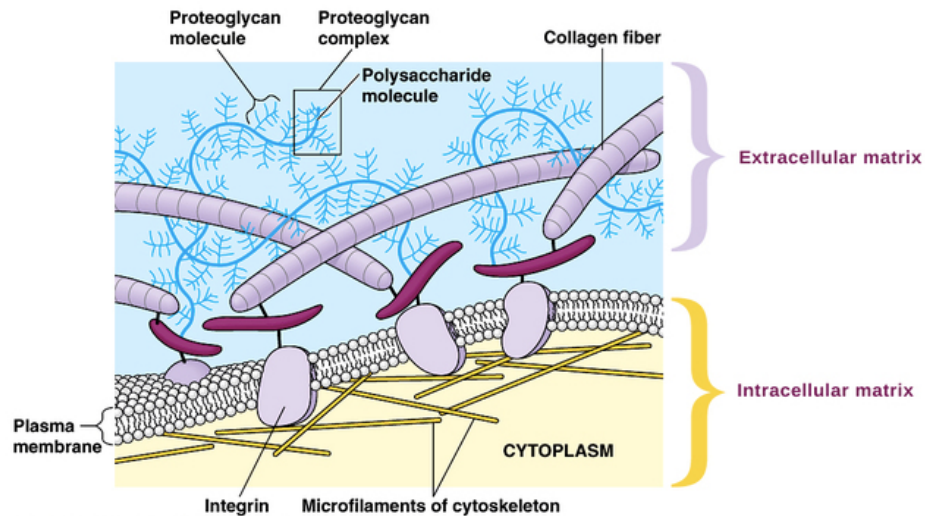
Figure 1: The ECM is a dynamic environment, and contains mechanical and biochemical signals for cells.[20] The ECM is composed of collagen fibers, polysaccharides and proteoglycan complexes.

1.3 The dynamic ECM

The ECM surrounding cells *in vivo* is not static, and changes in the biochemical environment help to regulate organ development and homeostasis, stem cell fate, tissue repair, and cancer initiation and progression.[1,10,20] For example, stem cells reside in specialized microenvironments called the niche, where the dynamic ECM helps balance quiescence, self-renewal and differentiation.[21,22] Disruption of this balance leads to tissue degeneration and aging. Dynamic changes in ECM composition leading to tumorigenic environments have been linked to several events in cancer initiation and progression including epithelial-mesenchymal transition, deregulation of stromal cell behavior, sustained proliferation, replicative immortality, angiogenesis, inflammation, avoidance of immune destruction, cancer cell invasion and metastasis.[10, 23] For *in vitro* evaluation of dynamic environmental changes on cellular activities, we require the ability to manipulate the biochemical properties of cell culture materials.

1.4 Hydrogel scaffolds for biomimetic ECM environments

Hydrogels are water swollen networks of polymers crosslinked through covalent bonds or physical interactions that mimic the structural network of the ECM.[8] Naturally occurring polymers (e.g agarose, alginate, chitosan, collagen, hyaluronic acid and hydroxyapatite) [24-29] and synthetic polymers (e.g. acrylamide, poly-ethylene glycol (PEG), polycarboxybetaine, POEGMA) [30-33] have been used as cell culture scaffolds. Some natural polymers are native to the ECM, and may possess an innate bioactivity. To fully control biochemical environments, the hydrogel must be composed of bio-inert

polymers that can be derivatized with bioactive ligands. Therefore, hydrogel polymers must also contain reactive sites for the introductive of bioactive molecules.

Hydrogels may be degradable, or non-degradable. Degradation commonly occurs through hydrolysis, enzymatic cleavage (e.g. cell secreted MMP) [34,35] or displacement of crosslinkers (e.g. calcium from alginate).[36,37] Non-degradable hydrogels, although less representative of *in vivo* conditions, provide a permanent structure to precisely control biochemical environments, whereas degradable hydrogels would alter the chemical environment over time. Therefore, this thesis will focus on the use of non-degradable hydrogels.

1.5 Controlling hydrogel pore size

Hydrogel porosity influences cell infiltration and migration. [24,38,39] Small pores (< ~1-5 µm) limit cell migration and may promote cell aggregation and necrosis. Because hydrogel pores are usually less than 1 µm, several strategies have been developed to create lager pores. Common methods include: (1) porogens [40]; (2) gas foaming techniques [41,42]; (3) controlling cross-linker type and density [43,44]; and, (4) photochemistry. [45]

(1) Porogens are degradable micro or nanoparticles embedded in hydrogels. [40,46] Alginate porogens are commonly used because large batches can be prepared in precise sizes, and are easily degradable by removal of the calcium cross-linker with EDTA. [47,48] Alginate can also be modified to be hydrolytically labile to increase particle degradation rates.

(2) Gas foaming creates pores by generating small gas pockets dispersed throughout the hydrogel. Foaming agents that slowly decompose into a gas are mixed into the polymer solution before gelation is initiated. [49,50] For example, sodium bicarbonate has been used to create pores in acrylic-acryl amide hydrogels as it decomposes into carbon dioxide. [51]

(3) The molecular weight and concentration of hydrogel components dictate pore size. For example, pore size of covalently crosslinked alginate hydrogels with poly(ethylene glycol) diamines was controlled by varying the molecular weight and weight fraction of the PEG diamines. [52]

(4) Hydrogels with photodegradable crosslinks have also been used to create well-defined pore size distributions using light. Multi-photon chemistry can spatially control pore sizes with 3D precision within the same hydrogel. [45,53]

1.5.1 Gelation mechanism

Hydrogels are formed by crosslinking polymers through covalent or non-covalent bonds to form a water swollen network. Gelation may be initiated by adding a crosslinker, changing the temperature (thermogelling), or irradiation with light.

(1) Covalent and non-covalent polymer crosslinkers. Hydrogels are commonly formed by mixing 2 polymers with corresponding reactive groups such as azide-DIBAC,[54] aldehyde-hydrazide,[55] thiol-maleimide or furan maleimide.[56,57]

(2) The crosslinks may be degradable or non-degradable. Non-degradable bonds are either reversible (e.g. diels-alder adduct)[58] or hydrolytically labile (e.g.

hydrazone).[59] Non-covalent bonds are formed through ion chelation or physical interactions such as alginate-$Ca2^+$ or host-guest chemistry, respectively.[60,61]

(3) Thermogelling hydrogels are a subcategory of non-covalent crosslinking hydrogels, dependent on temperature. For instance, agarose crosslinks through hydrogen bonds that form at low temperature.[24] Agarose is a naturally occurring polymer composed of disaccharide ((1→4)-3,6-anhydro-α-L-galactopryanosyl-(1→3)-β-D-galactopyranose) repeat units. The agarose units, D-galactose and 3,6-anhydro-L-galactopyranose, bind via covalent α-(1→3) and β-(1→4) glyosidic bonds. Once cooled, linear polymer chains aggregate through hydrogen bonds to form helical quasi rigid fibers, culminating in a three-dimensional mesh-like structure, which is stable at 37°C, whereas other polymers such as methylcellulose are liquids at low temperature, and gel upon heating.[62]

(4) Photochemical gelation forms covalent crosslinks between polymers, most commonly through a radical initiator.[63] For instance, polymers with methacrylate groups crosslink in the presence of a radical photoinitiator upon exposure to UV light.[64]

1.6 Biomolecule immobilization in hydrogels

Biomolecules such as peptides and proteins are immobilized in hydrogels to study cells in specific 3D biochemical environments.

1.6.1 Permanent immobilization methods

Permanent immobilization of biomolecules is achieved by reacting hydrogel functional groups with biomolecules to form non-degradable bonds.[65] Common strategies include nucleophilic addition, cycloadditions, photochemical reactions and high affinity physical interactions.

(1) Nucleophilic addition: Proteins and peptides are commonly immobilized though amino acid functional groups such as amines,[66] carboxylic acids,[67] and thiols.[68] Amines and carboxylic acids are reacted together through carbodiimide chemistry[66], and thiols are reacted with Michael acceptors[69]. Thiols are commonly reacted with maleimides to form a reversible bond; the ring must be hydrolytically opened to form the irreversible bond.[70] Nuttelman et al. modified poly(vinyl alcohol) (PVA) hydrogels with fibronectin to promote cell adhesion. An 11-carbon alkyl spacer was linked to PVA's hydroxyl groups via a stable ether linkage. The terminal acid group was activated with carbonyl imidazole (CDI for nucleophilic attack by amines on fibronectin. [66]

(2) Cycloaddition: Biomolecules are immobilized through Diels-Alder[71] and azide alkyne cycloadditions.[54,72] Diels Alder reactions are achieved commonly by reacting furans with maleimides because the cycloaddition occurs at 37° C or below. The biomolecule is usually modified with furans, and the hydrogel with maleimides, but the reversible is also possible. To increase reaction kinetics, the furan may be modified with electron donating groups.[73] Azide and alkyne cycloadditions require a copper catalyst or a highly reactive (strained)

alkyne.[72,74] Biomolecules and the hydrogel may be modified with the azide or alkyne.

(3) <u>Photochemical:</u> Light initiated photoreactions for biomolecule immobilization are typically achieved through photocages (protecting groups removed upon light exposure)[75,76] and radical reactions[77]. Light based immobilization in combination with multi-photon chemistry enables the creation of 3D biomolecule patterns within hydrogels.[78] Photocages can be cleaved to yield reactive groups for biomolecule grafting or for revealing bio-inert moieties to expose pre-immobilized biomolecules to cells[79]. Radical biomolecule grafting can be achieved by using vinyl polymerization or thiol-ene chemistry with photoinitiators.[80]

(4) <u>High affinity physical interactions</u>: For permanent biomolecule immobilization, only high-affinity non-covalent interactions such as streptavidin-biotin[81] and barnase-barstar[82] can be utilized, as weaker interactions can be easily disrupted. Proteins can be expressed with a biotin ligation sequence that is selectively biotinylated by the bacterial BirA ligase enzyme.[83] The biotinylated proteins are then immobilized in hydrogels modified with streptavidin.[84,85] Similarly, proteins can be expressed as barstar fusion proteins for immobilization in barnase modified hydrogels.[85]

1.6.2 Reversible immobilization methods

In an effort to mimic the dynamic environment, stimuli responsive materials have been investigated, including photochemical responsive polymers, non-covalent interactions, and reversible covalent bonds.[86] For hydrogels to accurately mimic the dynamic ECM, they must be amenable to multiple rounds of biomolecule immobilization (i.e., temporal patterning). Research has gradually progressed from static systems, to systems amenable to 1 round of immobilization/removal

(1) <u>Photochemical reversible immobilization</u>. Researchers have designed photoactive hydrogels where peptides can be immobilized and removed with light.[87] For example, RGD cell adhesive peptides that contained a nitrobenzyl linker were immobilized in PEG hydrogels through a photo-initiated thiol-ene reaction. Light was then used to cleave the nitrobenzyl linker, removing the RGD peptide from the PEG hydrogel network.[87] Deforest and Tirrell have developed a photoreversible protein-patterning system, where aldehyde-functionalized proteins are photo-reacted with and immobilized to alkoxy-amine containing hydrogels, forming a stable oxime ligation.[88] The proteins are then removed from the gel by cleaving a nitrobenzyl tether between the protein and gel polymer network with light. Proteins can re-immobilize until all the alkoxy-amines have been reacted.

(2) <u>Non-covalent interactions</u>. It has also been reported that peptides can be immobilized and removed using host-guest chemistry, where napththoic acid-modified RGD peptides were immobilized on an alginate surface coated with cyclodextrin. The naphthoic-RGD peptides were then removed by the addition of

the competitive adamantane-carboxylic acid-modified RGES, which has a higher affinity for cyclodextrin.[89]

(3) <u>Reversible covalent bonds</u>. Researchers demonstrated the ability to reversibly modify surfaces with the RGD peptide using reversible covalent bonds between phenylboronic acid (PBA) and 1,2/1,3-cis diols.[90] A glass slide was functionalized with PBA containing polymer brushes, and a modified RGD peptide conjugated with synthetic glycopolymer chains. The modified RGD was immobilized on the PBA modified substrate through multi-covalent interactions between the PBA groups in grafted polymer brushes, and the *cis*-diol groups in the glycopolymers. Addition and removal of the modified RGD was achieved by adding glucose or fructose, which triggered exchange with glycopolymer chains, allowing the release of RGD.

1.7 Current limitations

The systems described above are either only amenable to one round of biomolecule immobilization, require specialized equipment (e.g., photochemistry) or have only been demonstrated on 2D surfaces. To create a widely applicable method for dynamic biochemical environments, we require the ability to repeatedly exchange biomolecules over extended time periods with simple and translatable techniques.

2. Goal and Objectives

2.1 Goal:

Design *in vitro* cell culture scaffolds for the efficient exchange of biochemical

environments to temporally control biological activity.

2.2 Objectives:

1. Develop a reversible, user-friendly temporal patterning system for peptides in hydrogels.

2. Minimize time required for biomolecule immobilization and displacement

3. Demonstrate biological activity of dynamic biochemical environments

3. Results

3.1 Reversible temporal patterning system for peptides in hydrogels

We have developed a method to temporally control the biochemical composition of hydrogels by simply changing media composition. Biomolecules are immobilized through a strong but reversible interaction, and displaced by a second molecule that irreversibly binds to the biomolecule conjugate. This allows for the repeated and sequential immobilization of biomolecules to dynamically tune the chemical environment of surfaces or hydrogels. To demonstrate feasibility, we used the strong but reversible physical interaction between desthiobiotin and streptavidin (SA) and the irreversible interaction between SA and biotin (**Fig. 2**), which has previously been used to reversibly modify gold sensors.[92] Biomolecules are introduced as SA conjugates for immobilization and displacement.
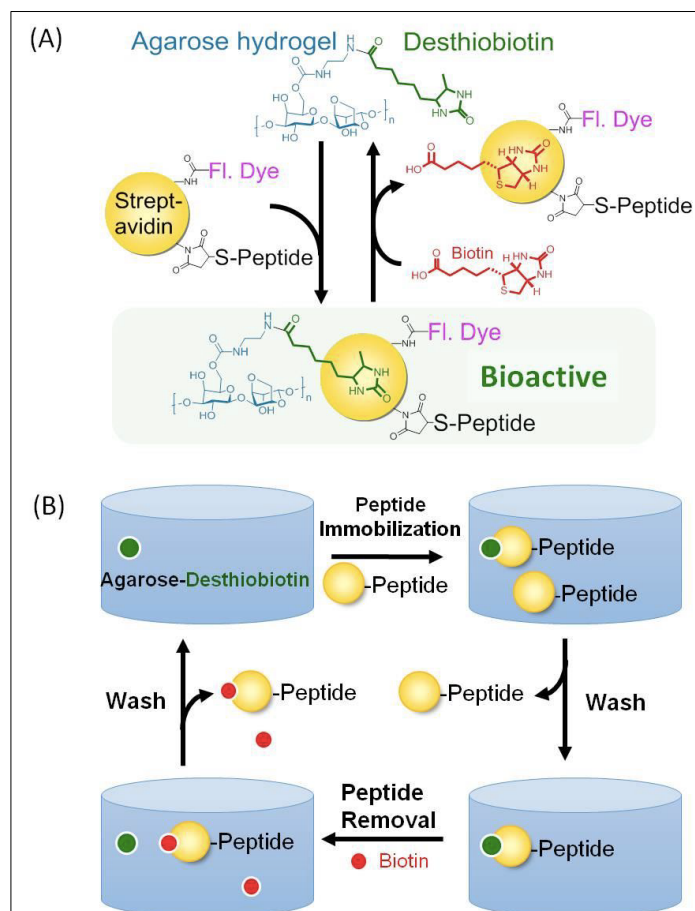
Figure 2: Schematic for the temporal control of biochemical environments in hydrogels. **(A)** Chemistry for the immobilization of SA-peptide conjugates in AgD hydrogels, and their displacement with biotin. **(B)** Procedure for the immobilization and displacement of SA-peptide conjugates in hydrogels including washing steps to remove unbound molecules.

To immobilize biomolecules, we synthesized SA-peptide conjugates by covalently linking a bioactive peptide to SA using thiol-maleimide chemistry. SA-RGD has previously been shown to increase cell adhesivity of surfaces.[92] Streptavidin-biomolecule conjugates formed between streptavidin and biotinylated growth factors are also bioactive[93], indicating biomolecules immobilized via streptavidin remain active. In

our system, addition of SA-peptide conjugates to desthiobiotin-modified agarose gels resulted in peptide immobilization. SA-peptide conjugates were displaced upon addition of biotin, which binds to SA with greater affinity than desthiobiotin (K_D of 10^{-15} M versus 10^{-11} M).[94] The newly formed biotin-SA-peptide complexes are then washed from the hydrogel to yield agarose-desthiobiotin (AgD) hydrogels that can be re-modified with the same or different peptide-SA conjugates. This system allows for multiple exchanges of the biochemical environment in hydrogels over time.

3.1.1 Synthesizing AgD
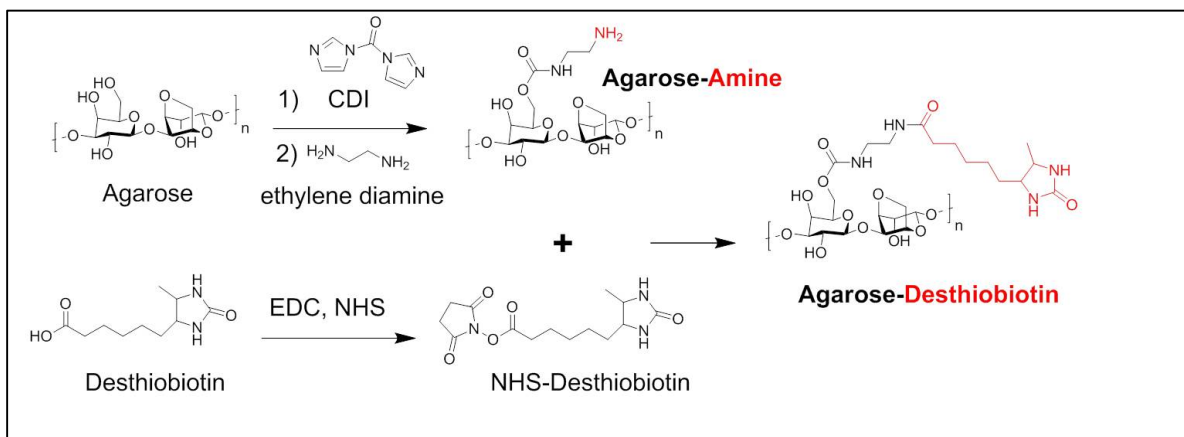
Figure 3: Synthesis of AgD from agarose and NHS-desthiobiotin.

To synthesize AgD, we first made agarose-amine and *N*-hydroxysuccinimide desthiobiotin (NHS-desthiobiotin). Agarose-amine was synthesized by reacting agarose with carbonyldiimidazole (CDI) followed by an excess of ethylene diamine. After purification by dialysis and isolation by freeze drying, agarose-amine was reacted with NHS-desthiobiotin to yield AgD (**Fig. 3**).

The degree of amine and desthiobiotin functionalization on agarose was determined using a fluorescamine assay with N-(2-aminoethyl) acetamide as the amine standard. Agarose-amine had an amine substitution rate of 4.4 ± 0.3 µmol of amines per mmol of agarose repeat units (mean ± standard deviation, n=3). AgD retained 3.0 ± 0.5 µmol of amines per mmol of agarose (mean ± standard deviation, n=3). Because the decrease in primary amine content is due to desthiobiotin conjugation, a substitution rate of 1.4 ± 0.6 µmol of desthiobiotin per mmol of agarose subunit (mean ± standard deviation n=3) was estimated. The Thermo Scientific Fluorescence Biotin Quantitation assay was used to directly confirm desthiobiotin content, which yielded a substitution rate of 1.7 ± 0.5 µmol desthiobiotin per mmol of Ag subunit (mean ± standard deviation n=3, **Fig. S1A**), which was not significantly different from the fluorescamine assay estimate (unpaired t test, $p < 0.05$).

3.1.2   Synthesis of SA-peptide conjugates
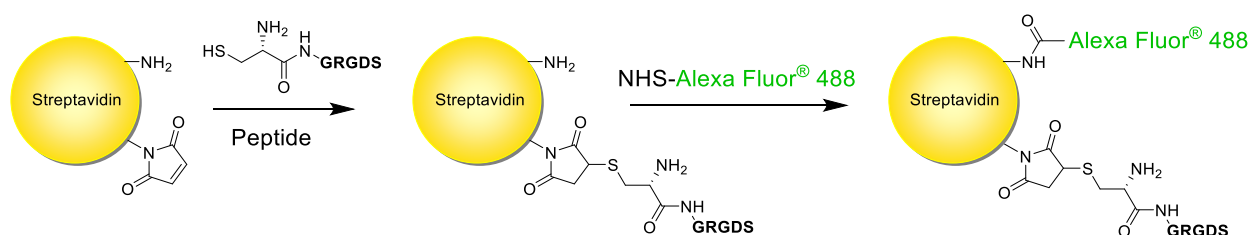
Figure 4: Synthesis of SA-RGD by reacting maleimide-SA with CGRGDS and NHS-Alexa™ Fluor 488.

SA-RGD-488 was synthesized by reacting maleimide-SA with CGRGDS in PBS pH 7.4 for 2 hours. SA modified with CGRGDS was then reacted with NHS-Alexa 488 to yield SA-RGD-488. The degree of Alexa 488 labelling was quantified by UV-Vis, and

determined to be 1.4 Alexa 488 molecules per SA. The reaction of CGRGDS with maleimide-SA was confirmed by MALDI-TOF/TOF before modification with Alexa 488. The reaction resulted in a mixture of 1 and 2 CGRGDS peptides per streptavidin monomer, which results in 4 to 8 CGRGDS peptides per streptavidin tetramer **(Fig. S2).**

3.1.3 Reversible binding of fluorescently labelled SA in PBS/BSA solutions

To demonstrate SA conjugate binding to AgD gels, unmodified agarose and AgD gels were incubated in SA-488 solutions. Gels were rinsed in PBS to remove any excess, unbound SA-488 conjugates. After 30h of rinsing in PBS, fluorescence readings from unmodified Ag gels (n=6) approached zero, suggesting that removal of free SA-488 was complete (**Fig. 5A**). Fluorescence readings from AgD gels (n=6, t=4 to 48h, **Fig. 5A**) corresponded to an average SA concentration of 0.222 ± 0.007 μM. The decrease in fluorescence between the 4 and 48h time points was not statistically significant (unpaired t test, $p < 0.05$), indicating that most of the SA-488 remained in the gels. A set of SA-488 bound AgD gels (n=16) were left in the PBS rinsing solution to determine long-term stability of immobilized SA-488, and no significant change in fluorescence occurred between day 13 and day 61 of rinsing (unpaired t test, $p < 0.05$) (**Fig. S4**). Fluorescence profile as a function of depth was quantified in ~ 1.1 mm thick hydrogels (**Fig. S5**), and showed a decrease in fluorescence of 59% of the entire gel. The fluorescence from the meniscus to the bottom of the gel (~0.25 to 1.1 mm) is linear with an equation of the line of $y = -57.5x + 93$ with an R-squared of 0.994. This is expected since SA-488 was soaked into the gel from the surface. Little variation occurs over the first 100 μm, which is near

the maximum thickness for cell-hydrogels constructs due to the limitation of oxygen and nutrient diffusion. From the maximum fluorescence at bottom of the meniscus at 0.25 mm in **Fig. S5** to 0.35 mm, the fluorescence intensity decreased by ~4%.

When gels were exposed to a PBS/BSA solution containing a large excess of biotin (t=48 h, **Fig. 5A**), fluorescence readings decreased suddenly, reaching a SA-488 concentration of 0.017 ± 0.001 µM after 48 h of biotin exposure (t=96 h, **Fig. 3A**), a decrease of 92%. This demonstrates that biotin displaced SA-488 from AgD hydrogels.

To demonstrate sequential immobilization, excess biotin was rinsed from the gels (t=96 h to t=132.5 h, **Fig. 5A**), which were then re-exposed SA-488. The fluorescence from unmodified agarose gels rapidly returned to baseline once exposed to the rinsing solution while AgD gels retained SA-488 (0.27 ± 0.01 µM, t=152.2 to 196 h, **Fig. 5A**). Addition of biotin (t=196h, **Fig. 5A**) decreased the concentration of SA-488 to 0.033 ± 0.002 µM (t=228h, **Fig. 3A**). A third immobilization-displacement step within the same gels yielded similar results, with 0.25 ± 0.01 µM SA-488 immobilized within AgD gels (t=320 to 364h, **Fig. 5A**), and 0.026 ± 0.002 µM of SA-488 after biotin exposure (t=414h, **Fig. 5A**). The average concentration of immobilized SA-488 in the three repetitions prior to biotin exposure was 0.25 ± 0.02 µM. These results demonstrate that AgD gels can predictably bind and release SA conjugates with temporal control.

To demonstrate sequential immobilization of different SA conjugates, a parallel experiment was performed exposing agarose (n=6) and AgD (n=3) gels to both SA-488 and SA-647 (**Fig. 5B**). The gels were first exposed to SA-488. 0.228 ± 0.007 µM SA-488 remained in the AgD gels, and dropped to 0.0106 ± 0.0008 µM after exposure to biotin.

After rinsing away excess biotin, the gels were exposed to SA-647; 0.18 ± 0.01 µM remained in the AgD gels, with residual SA-488 levels dropping to 0.0105 ± 0.0002 µM during biotin exposure. Finally, the gels were exposed to both SA-488 and SA-647 simultaneously, yielding concentrations of 0.250 ± 0.009 and 0.232 ± 0.008 µM respectively; both dropped to 0.016 ± 0.002 µM after biotin displacement. These results demonstrated that the AgD gels can sequentially and simultaneously immobilize a variety of SA conjugates. Biotin displacement dropped the concentration of SA conjugates in the hydrogels by an average of ~92% in PBS/BSA conditions (**Fig. 5A and B**). SA immobilization was also directly proportional to the amount added to the hydrogels.

AgD gels simultaneously bound different fluorescent SAs with immobilized concentrations proportional to feed ratios. Gels were exposed to a combined concentration (0.01 mg/mL) of two different fluorescent SAs at varying ratios in PBS/BSA (**Fig. 5C**). SA-488 to SA-647 ratios of 3:1, 1:1, and 1:3 resulted in the immobilization of 0.16 ± 0.01 µM SA-488 and 0.054 ± 0.004 µM SA-647, 0.11 ± 0.01 µM of both SA-488 and SA-647, and 0.08 ± 0.01 µM SA-488 and 0.204 ± 0.007 µM SA-647, respectively. The average combined immobilized SA concentration in each ratio was 0.24 ± 0.02 µM, similar to previous experiments with 0.01 mg/mL SA feeds (**Fig. 5A-B**). The third immobilization round **in Fig. 5B** yielded bound concentrations of 0.250 ± 0.009 and 0.232 ± 0.008 µM from a solution of 0.01 mg/ml of both SA-488 and SA-647.
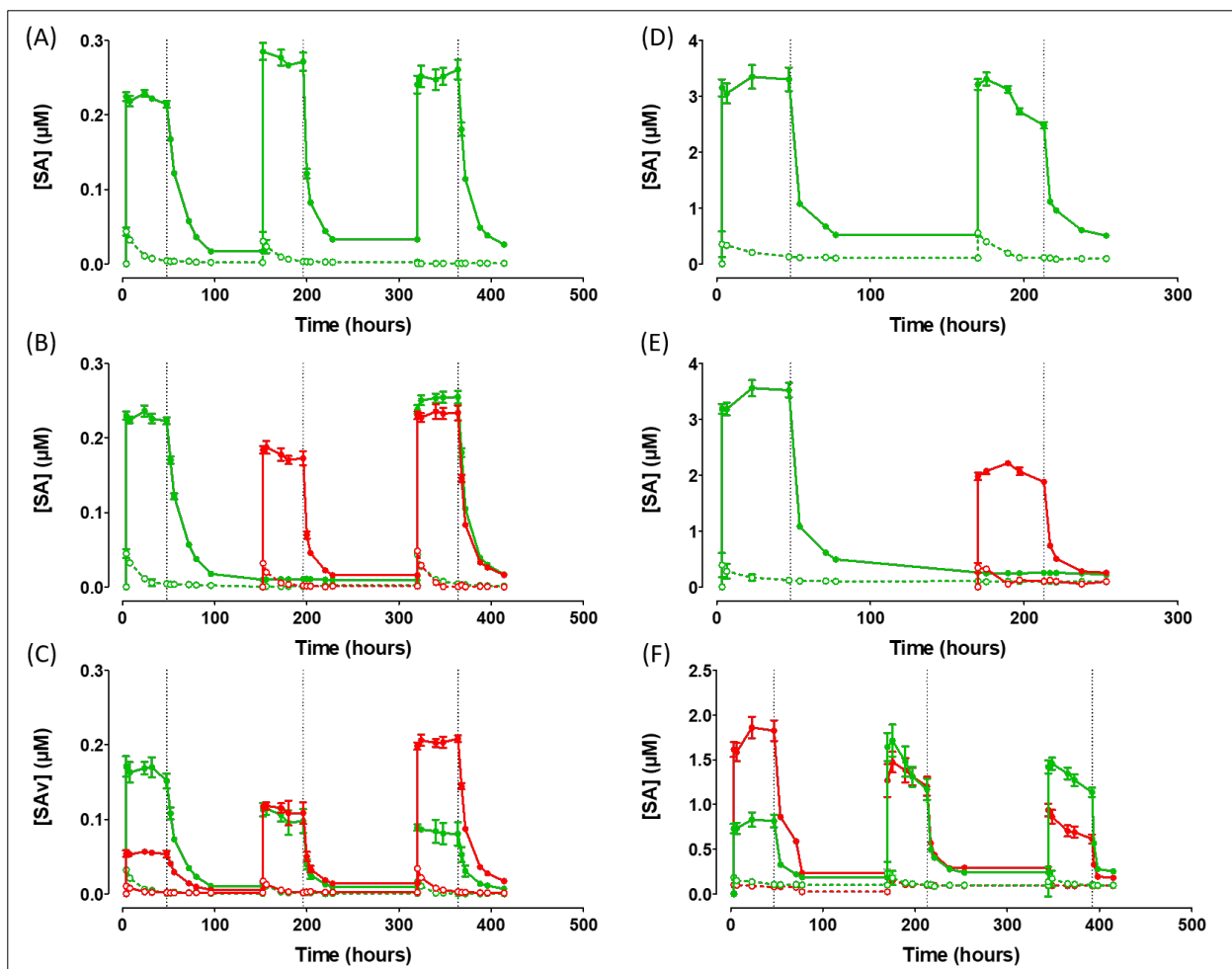
Figure 5: Sequential and simultaneous immobilization of SA-488 (green) and SA-647 (red) within 0.7 wt.% AgD (solid lines) and agarose (dashed lines) hydrogels in PBS with BSA (A-C) and PBS with 1% CBS (D-F). (A) 50 µL of 0.01 mg/mL of SA-488 was added to the gels at 0, 152 and 320 h and displaced by biotin (indicated by dashed lines) at 48, 196 and 364 h (mean ± standard deviation, n = 3 for AgD and n = 6 for agarose). (B) 50 µL of 0.01 mg/mL SA-488 was added at 0 and 320 h, 50 µL of 0.01 mg/mL SA-647 was added at 152 and 320 h, and biotin at 48, 196 and 364 h (mean ± standard deviation, n = 4 for AgD and n = 6 for agarose). (C) To control relative SA concentrations, gels were exposed to solutions containing 0.01 mg/ml of SA-488:SA-647 ratios of 3:1, 1:1 and 1:3 at times 0, 152 and 320 h, respectively. Biotin was added at 48, 196 and 364 h

(mean ± standard deviation, n = 6 for AgD and agarose). (D) 50 μL of 0.1 mg/mL of SA-488 was added at 0 and 170 h and displaced by biotin at 47 and 213 h (mean ± standard deviation, n = 4 for AgD, and n = 3 for agarose). (E) 50 μL of 0.1 mg/mL of SA-488 was added at 0 h, 50 μL of 0.1 mg/mL of SA-647 at 170 h, and biotin at 47 and 213 h (mean ± standard deviation, n = 4 for AgD and agarose). (F) Solutions of 0.1 mg/ml SA-488:SA-647 ratios of 1:3, 1:1 and 3:1 were added at 0, 170 and 344.5 h, respectively. Biotin was added at 47, 213 and 392 h (mean ± standard deviation, n = 4 for AgD and n = 3 for agarose). Agarose gels without desthiobiotin (Ag) showed minimal binding.

3.1.4 Reversible binding of fluorescently labelled SA in PBS with serum

CBS did not interfere with the immobilization and displacement of fluorescent SAs. SA-488 bound to AgD gels with 0.1 mg/mL SA solutions in 1% CBS, exhibiting a bound concentration of 3.2 ± 0.2 μM before decreasing to 0.52 ± 0.02 μM after biotin exposure (**Fig. 5D**). A second exposure to SA-488 immobilized 3.0 ± 0.3 μM, and decreased to 0.50 ± 0.01 μM after biotin displacement. A parallel experiment using SA-488 followed by SA-647 gave an initial concentration of 3.4 ± 0.2 μM for SA-488 that decreased to 0.26 ± 0.01 μM after biotin displacement, followed by retention of 2.0 ± 0.1 μM of SA-647 that decreased to 0.255 ± 0.005 μM after biotin exposure (**Fig. 5E**). In 1% CBS solutions, an average SA concentration of 2.9 μM was immobilized, and biotin displaced ~87% of bound SA. Immobilized SA was directly proportional to amount of SA added with 0.01 (**Fig. 5A-B**) or 0.1 mg/ml (**Fig. 5D-E**) immobilizing 0.23 and 2.9 μM, respectively. To investigate tolerability of common cell culture serum concentrations (1-10%), a 10% CBS control was investigated and confirmed that immobilization and

displacement is not dependent on serum concentration. The relative fluorescence of SA-488 in 1 and 10% CBS tracked very similarly in AgD gels for both 117 h before and 74.5 h after biotin addition. The simultaneous binding of different SAs was also confirmed in 1% CBS (**Fig. 5F**), where the combined concentration of immobilized SA was 2.2 μM. The ratio of SA conjugates immobilized was directly proportional to the ratio of SA conjugated added (**Fig. 5C,F**).

3.1.5 Immobilization and displacement of SA-RGD

SA-RGD was immobilized and displaced in AgD gels with 1% CBS. In the first step, only SA-RGD was immobilized resulting in a concentration of ~0.64 μM (**Fig. 4**). The binding of SA-RGD is less efficient than SA-488 by approximately a factor of 4, which may be attributable to the larger and more sterically hindered SA-RGD. Then SA-RGD and SA-647, a surrogate for another bioactive molecule, were simultaneously immobilized at different ratios SA-RGD:SA-647 (3:1 and 1:3), demonstrating the ability to temporally control the biochemistry/biochemical properties of hydrogels using a bioactive peptide.
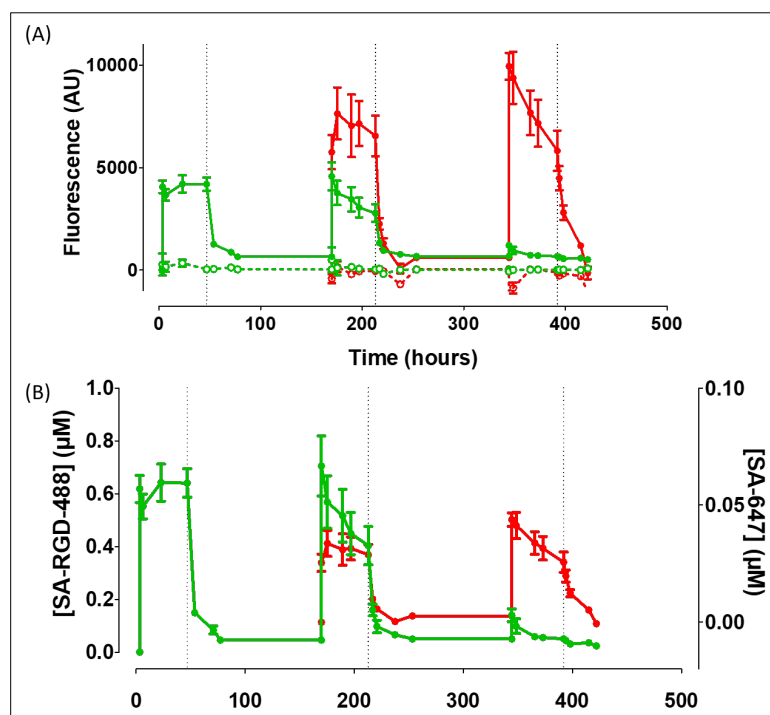
Figure 6: Immobilization of SA-RGD-488 (green) and SA-647 (red) in AgD (solid line) and agarose (dashed line) hydrogels in PBS with 1% CBS. Three rounds of immobilization were performed as follows: (1) 50 µL of 0.1 mg/ml SA-RGD-488 was added at 0 h and biotin at 47 h; (2) 50 µL of 0.1 mg/ml of total SA concentration with a 1:3 SA-RGD-488:SA-647 was added at 170 h and biotin at 213 h; and, (3) 50 µL of 0.1 mg/ml of total SA concentration with a 3:1 SA-RGD-488:SA-647 was added at 344.5 h and biotin at 392 h. (A) Fluorescent measurement of the gels to track SA-RGD-488 and SA-647 immobilization and displacement. (B) Fluorescence from (A) was converted into SA concentration using calibration curves (mean ± standard deviation, n=3 for AgD and n=4 for agarose).

3.2   Decreasing the time required for exchanging biochemical environments

Ideally, chemical environments should be rapidly exchanged to study cells in dynamic environments. Our process is limited by the diffusion of SA conjugates and biotin. The time for chemical exchange was reduced by decreasing hydrogel volume, increasing the surface-area to volume ratio and controlling pore size in the hydrogel.

3.2.1   Immobilization of hydrogels on glass slides

To decrease gel size and increase media contact area, we immobilized AgD gels on the surface of microscope slides. Glass slides were cleaned in a 3M KOH bath, subsequently washed with water and dried overnight. A 1.5% hydroxyl(polyethyleneoxy)propyl triethoxysilane solution (provided by Prof. Mike Brook) in dry methanol was applied and spin coated on the surface of a cleaned glass slide (**Fig. 7**). After drying for 4 hours, the slides were placed in 15 mL of a 5 mg/mL CDI solution in DCM for 24 hours. Slides were rinsed with DCM and dried again at 95ºC for 4 hours. Hydrophobic circles with an inner diameter of 5 mm were created on the slides using a PAP pen. Then, 20 µL of a 10 mg/mL AgD, which contains primary amines, solution in PBS was pipetted within the hydrophobic circles (**Fig. 8).** Gelation was initiated by placing the slides at 4° C for 60 minutes.
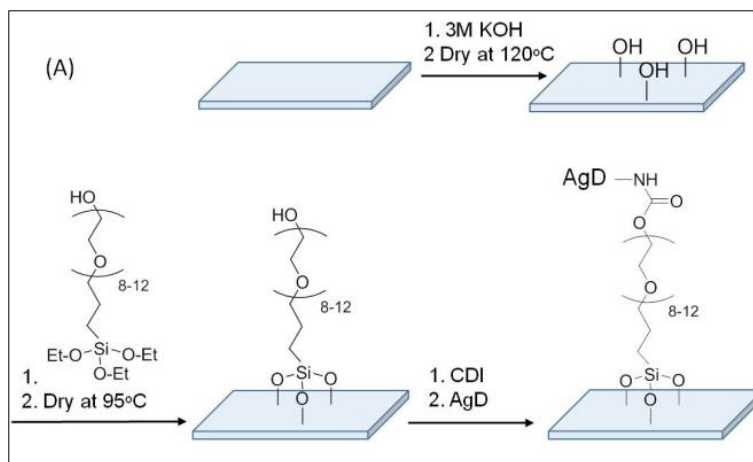
Figure 7: Functionalizing glass slides with HO-PEG10-Si(OEt)$_3$ for immobilization AgD hydrogels.
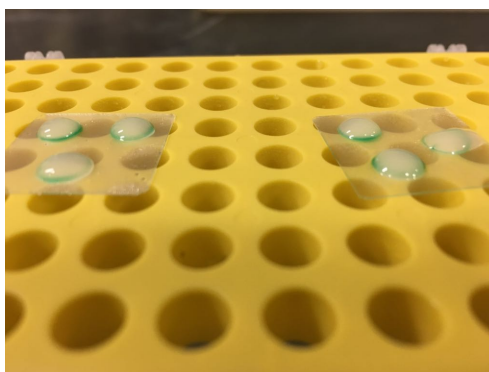
Figure 8: 20 μL AgD hydrogels immobilized on glass slides.

3.2.2 Biochemical exchange in 20 *μ*L AgD gels immobilized on glass

The time required for biochemical exchange in AgD hydrogels was determined by immobilizing and displacing SA-488. First, 40 μL of a 0.01 mg/mL SA-488 solution in PBS was pipetted on top of the gels, and incubated overnight. Removal of unbound SA-488 and biotin displacement of SA-488 was conducted in 200 mL of PBS with 0.5 mg/mL of BSA and PBS with 0.5 mg/mL of biotin and BSA, respectively. Hydrogel

37

fluorescence was quantified using fluorescence microscopy, and images were analyzed in ImageJ using identical square sections in multiple hydrogels. Agarose-desthiobiotin gels not exposed to SA-488 were used as blanks.
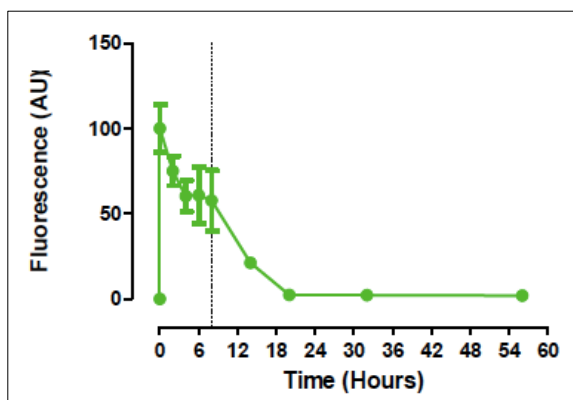
Figure 9: The fluorescence time profile of SA-488 immobilized in and displaced from 20 μL AgD hydrogels conjugated to silane functionalized glass slides. Dashed line indicates the addition of biotin.

We can observe from **Figure 9** that excess SA-488 was removed from the gel within 4 hours, whereas 30 hours was required for 60 μL AgD gels. Biotin displacement of SA-488 from the gel occurred within 12 hours, compared to 48 hours for the 60 μL gels. This represents an improvement of 75% improvement for the displacement of SA-488.

3.2.3 Controlling hydrogel pore size with alginate porogens

The pore size of AgD hydrogels were increased to further reduce the time required for biochemical exchange. Alginate porogens were incorporated in AgD

hydrogels to control pore size distribution. Two different porogen sizes were fabricated in large batches from an emulsion technique.

3.2.4 Fabrication of alginate microparticles (porogens)

Alginate microparticles were prepared following an emulsification/internal gelation protocol developed by Reis et al.[47] An aqueous dispersion of insoluble calcium carbonate crystals (5% w/v) was sonicated for 30 minutes in milliQ water to dissolve aggregated crystals. Then, 8.3 mL of the calcium carbonate mixture was mixed with 50 mL of a 2wt% alginate solution in water. After 15 minutes of mixing at 500 rpm (mechanical stirrer with propeller), 50 mL of paraffin oil containing 1.5 mL of Span 80 was added. The mixture was emulsified at 1600 rpm for a further 15 minutes. 20 mL of paraffin oil containing 830 μL of glacial acetic acid was added, followed by stirring for an additional 60 minutes at 1600 rpm (for 10-20 μm particles) and 250 rpm (for 80-100 μm particles, **Fig. 11**).

Particle were recovered by centrifugation and washed with mixtures of acetone/hexane/isopropanol to remove residual oil. Particles were washed 6 times in the solvent mixtures and centrifuged at 15,000 x g. Alginate microparticles still contained oil as demonstrated by the addition of a hydrophobic fluorescent dye, Nile red. A Tween 20/$CaCl_2$ mixture was used to remove residual oil (**Fig. 10).**
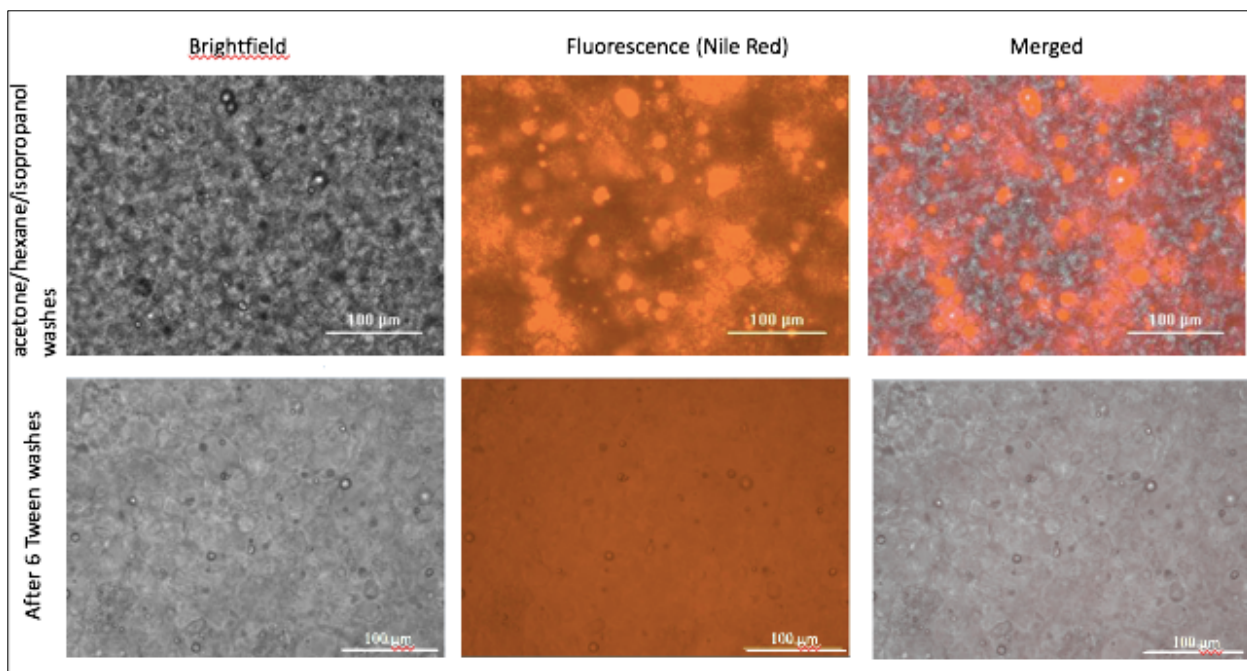
Figure 10: Confirmation of oil removal from alginate microparticles by visualization of oil droplets with Nile Red. The first row are images of particles after washing with a Triton X 100 and CaCl$_2$ mixture. To completely remove residual oil, particles were washed with Tween (bottom row).
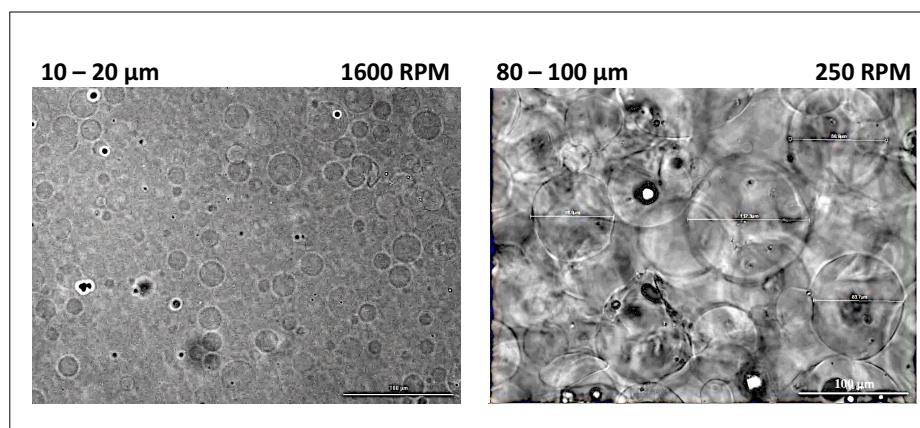
Figure 11: Mixing speeds during emulsion influenced alginate particle size. Smaller particles (10-20 μm) were formed are faster mixing speeds.

3.2.5 Controlling pore size in AgD hydrogels with alginate porogens

Alginate porogens were incorporated in AgD hydrogels, and degraded with EDTA. First, alginate microparticles were centrifuged and pelleted to volume of 200 μL. Then, 200 μL of AgD was added to the pelleted alginate microparticles. After mixing, the alginate and AgD mixture was pipetted into a 96 well cell culture plate, in 60 μL volumes. The mixtures were placed in the freezer for rapid gelation. A 0.5 M EDTA solution was then pipetted on top of the hydrogels to degrade the alginate porogens.

Once the alginate microparticles were degraded, the porous AgD hydrogels were labelled with 0.1 mg/mL SA-488. The experiment was conducted using both, 10-20 μm sized particles and 80-100 μm sized particles. Confocal microscopy was used to visualize the pores (**Fig. 12).**
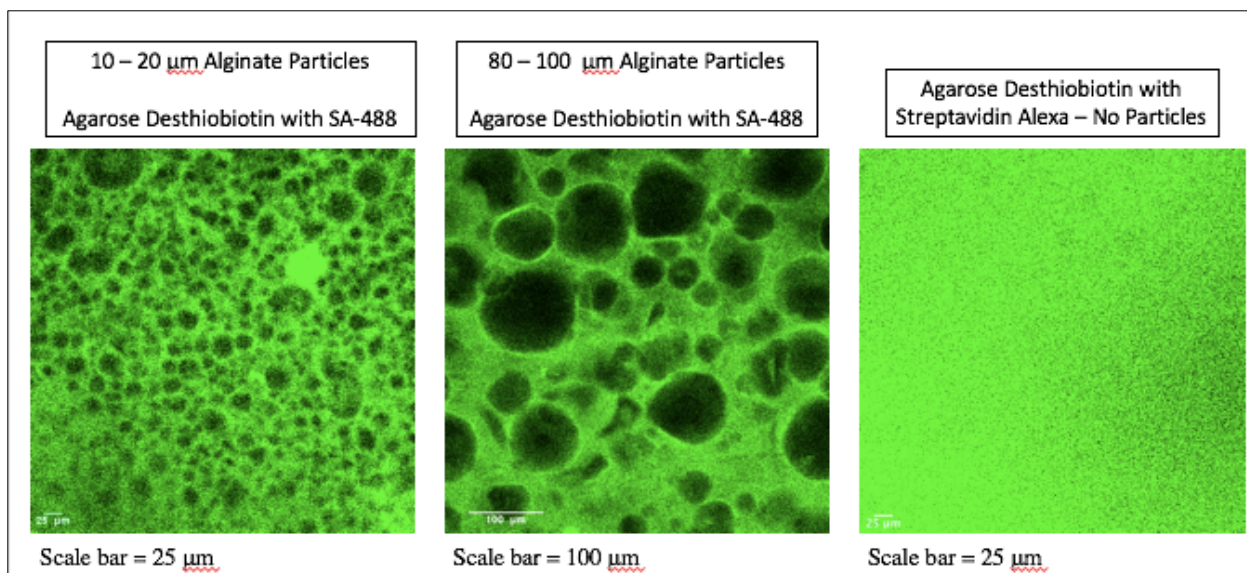
Figure 12: Confocal images of non-porous and porous AgD hydrogels labelled with SA-488 constructed with 10-20 μm and 80-100 μm alginate particles. Dark spaces indicate pores.

3.2.6 Porous hydrogel binding studies in PBS and serum conditions

To investigate biochemical exchange in porous (10-20 μm) AgD hydrogels, we compared SA immobilization and displacement in: (1) 60 µL porous AgD hydrogel in PBS/BSA in a 96 well cell culture plate; (2) 60 µL porous AgD hydrogel in PBS/CBS in a 96 well cell culture plate; and, (3) 20 µL porous AgD hydrogel in PBS/BSA on a glass slide. The time required to displace immobilized SA-488 with biotin from AgD gels was determined to be 5.67, 3.33 and 4.67 hours for 60 µL gels in PBS, 20 µL gels in PBS, and 60 µL gels in CBS (**Fig. 13**).
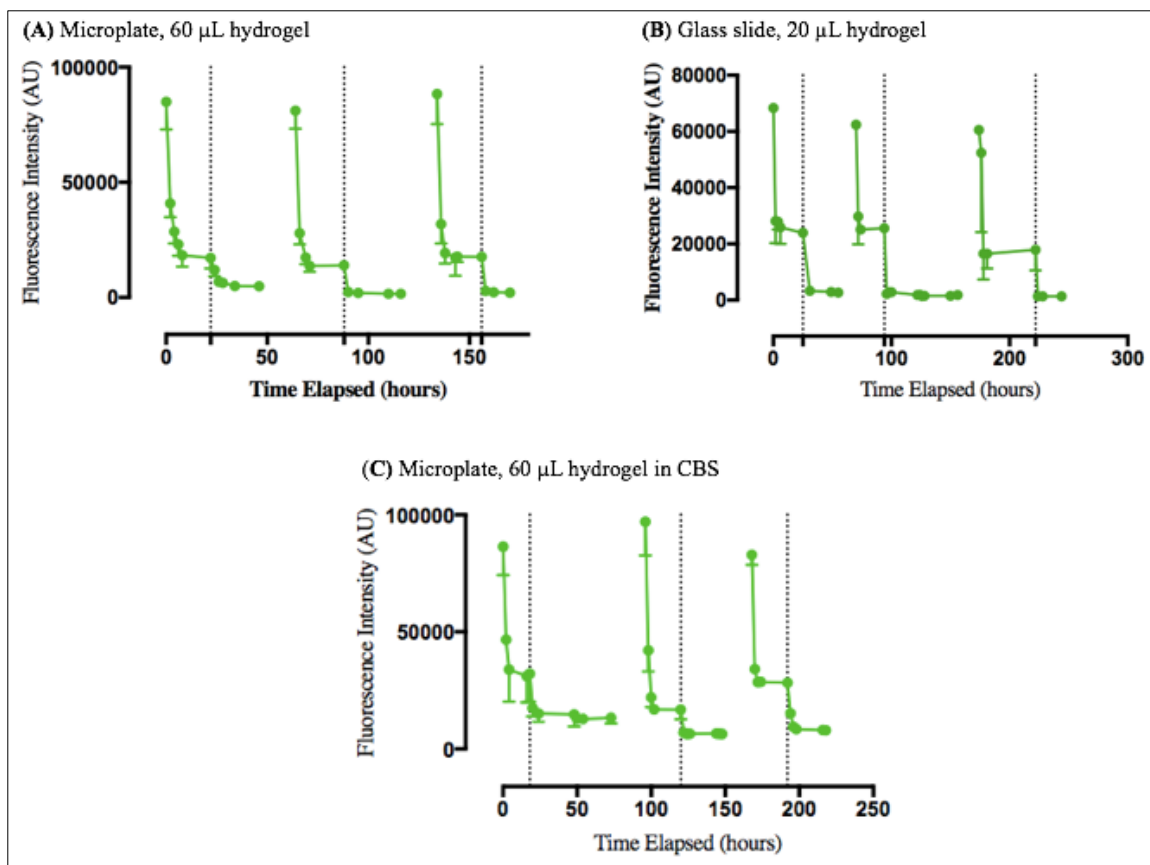
Figure 13: Porous hydrogel binding studies with SA-488. Dotted lines indicate addition of 0.5 mg/mL biotin and BSA. **(A)** 60 µL porous AgD gels in PBS with BSA (in 96 well plate). **(B)** 20 µL porous AgD gels on glass slides in PBS with BSA. **(C)** 60 µL porous AgD gels in 1% CBS (in 96 well plate).

3.3 Bioactive AgD gels with reversible biochemical environments

We demonstrated the ability to influence human umbilical vein endothelial cell (HUVEC) tube formation with a dynamic biochemical environment, and the ability to seed cells into AgD gels with larger pores.

3.3.1 SA-RGD bioactivity and HUVEC tube formation on temporally controlled biochemical environments.

HUVECs plated on AgD gels with and without SA-RGD showed different adhesion properties. Without SA-RGD, HUVECs clustered and maintained a circular morphology (circularity: 0.96±.08; **Fig. 14A, C**). AgD gels with SA-RGD encouraged the attachment and spreading of HUVECs within 3h (**Fig. 14B**), with a circularity of 0.61±.17 which was significantly different from HUVECs on AgD gels (unpaired t-test p < 0.01, **Fig. 14C**). Biotin was added to the media of some AgD gels with SA-RGD after 4 h of culture. After 6 h (2 h since biotin addition), HUVECs on AgD with SA-RGD, and SA-RGD with biotin showed initial signs of tube formation (**Fig. 14E-F**). After 24 h, HUVECS formed large clusters on gels without SA-RGD (**Fig. 14G**). Gels with SA-RGD formed large tube structures (**Fig. 14H**), contrasted by smaller tube structures on gels with SA-RGD and biotin (**Fig. 14I**). Cells were stained with Calcein AM after 30 h to highlight differences in tube formation between SA-RGD and SA-RGD with biotin samples. Gels with SA-RGD showed large tube structures (**Fig. 14K, M and N**), whereas gels with SA-RGD and biotin demonstrated smaller tube formations (**Fig. 14L**). Total tube length per gel was 3380±517 μm for SA-RGD, and 1340±545 μm for SA-RGD with

biotin conditions (**Fig. 14O**, one-way ANOVA Tukey's post hoc test, $p < 0.01$). SA-RGD

modification of AgD gels encouraged HUVEC adhesion, and displacement of SA-RGD

with biotin after 4h hindered tube formation, demonstrating that temporal biochemical

environments influence HUVEC tube formation.
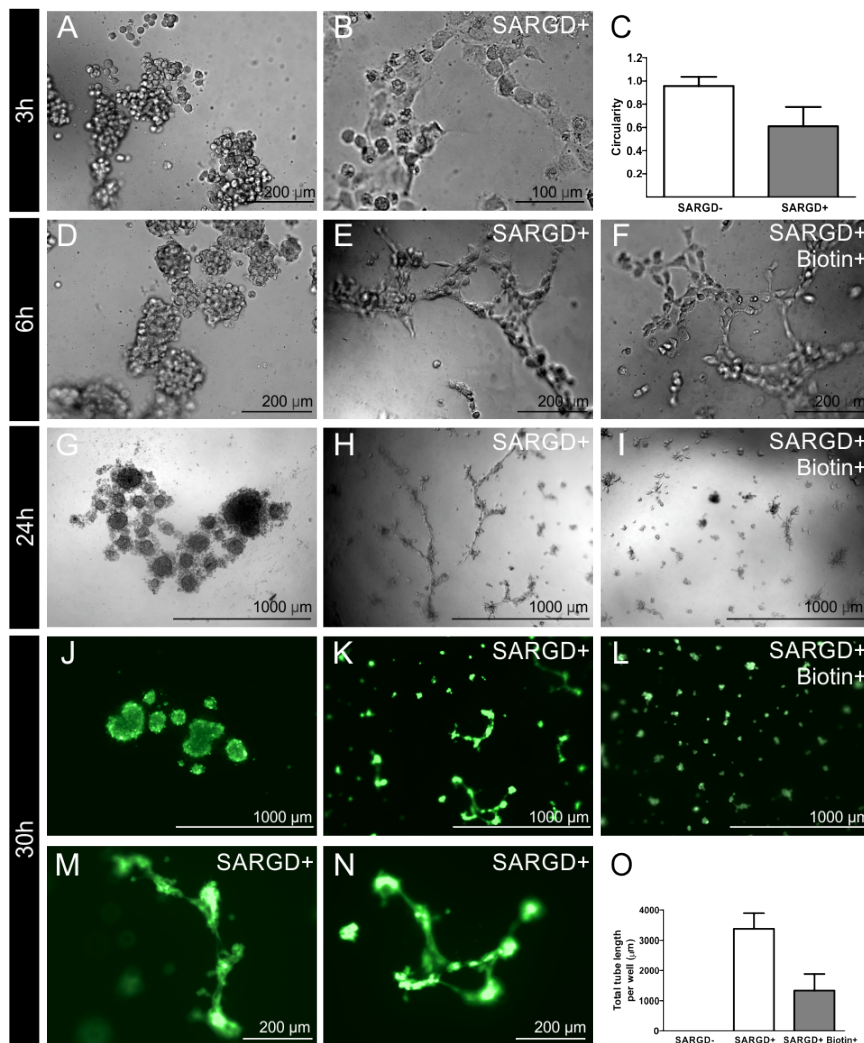
Figure 14: HUVEC adhesion and tube formation with temporal biochemical environments.

HUVECs only adhered to AgD gels modified with SA-RGD (A, B), as evidenced by a decrease

in cell circularity (C, mean ± standard deviation, n=3). Biotin was added to 3 gels with SA-RGD

after 4 h. After 6 h, HUVECS still did not adhere to gels without SA-RGD (D), and gels with SA-RGD (E) and SA-RGD + biotin (F) showed similar HUVEC adhesion and morphology. After 24 h, HUVECs clustered on the surface of AgD gels (G), formed large tube structures on SA-RGD AgD gels (H), and smaller tube structures on AgD gels with both SA-RGD and biotin (I). After 30 h, cells were stained with Calcein AM. HUVECs remained clustered on the surface of AgD gels (J), contained large tube networks on AgD gels with SA-RGD (K, M, N) and smaller tube structures on AgD gels with both SA-RGD and biotin (N). Total tube length per gel was quantified in image J (O, mean ± standard deviation; n=3) and gels with SA-RGD showed greater tube formation than AgD gels with SA-RGD and biotin (p<0.01).

3.3.2 Seeding fibroblast cells into porous AgD hydrogels modified with SA-RGD
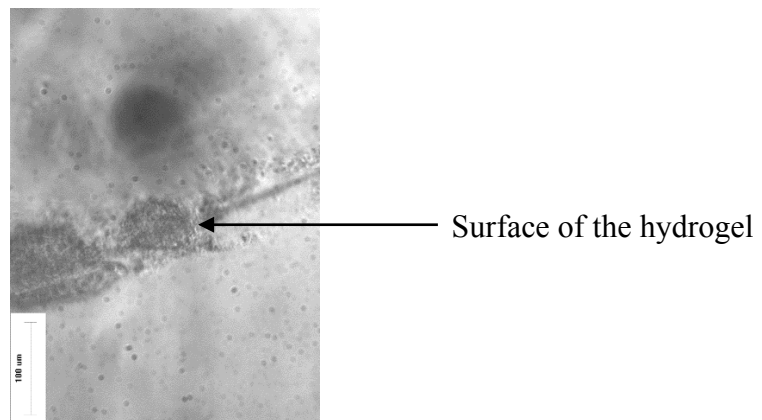
Figure 15: Neural stem cells were seeded onto a 0.5% agarose hydrogel mostly remained on the surface of the gel.

Porous agarose hydrogels improve cell infiltration. As shown in **Figure 15**, neural stem cells do not efficiently infiltrate 0.5 wt% agarose hydrogels (pore size of ~100 nm [24,95]) modified with RGD. 0.5 wt% agarose is the lowest practical concentration for cell culture due to stability limitations. To demonstrate cell seeding into agarose gels with

larger pores, we modified porous (10-20 μm porogens) 60 μL AgD hydrogels with SA-RGD and seeded fibroblasts. After 24 h, cells were stained with Calcein and visualized. Cells were visible throughout the gel as demonstrated by fluorescent image slices from a z-stack **(Fig. 16A)**. Cells were also found adhered to the bottom of the well, indicating migration through the entire gel **(Fig. 16B)**.

Depth: 91.2 µm   Depth: 230 µm   Depth: 316.8 µm   Bottom of well
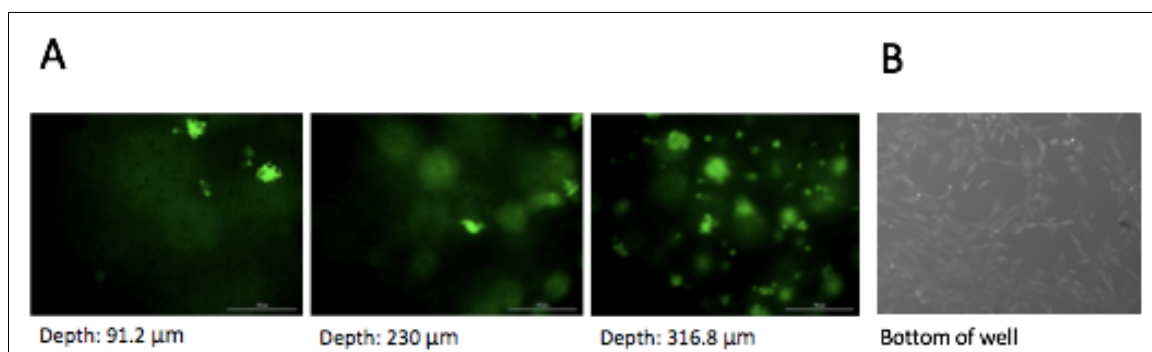
Figure 16: (A) Confocal images from a 541 µm tall AgD hydrogel labelled with SA-RGD seeded with fibroblasts. Cells localized throughout the gel indicating the pores allowed cell migration. **(B)** Mouse fibroblast cells that migrated through porous AgD hydrogels, and adhered to the bottom of the well.

3.3.3 AgD hydrogels are non-cytotoxic

To evaluate cytotoxicity, 10,000 fibroblasts were seeded onto 3 different hydrogels: (1) agarose gels; (2) AgD gels modified with SA-RGD; and, (3) porous AgD gels modified with SA-RGD **(Fig. 17)**. After 1 day of culture, cells were analyzed with a viability assay (CellTiter 96® AQ$_{ueous}$ One Solution Cell Proliferation Assay (MTS)). Bio-inert agarose gels without any modification were used as the non-cytotoxic control. AgD gels modified with SA-RGD had higher cell viability than agarose gels due to RGD

promoted adhesion, and proliferation. Porous SA-RGD AgD and non-porous agarose gels had similar cell viability, and but both gels had lower viability than non-porous SA-RGD AgD gels. Therefore, the porous gels were non-cytotoxic but did not promote the same level of cellular activity as non-porous gels. This is most likely due to differences between 2D and 3D environment, which has been shown to influence cellular activity.
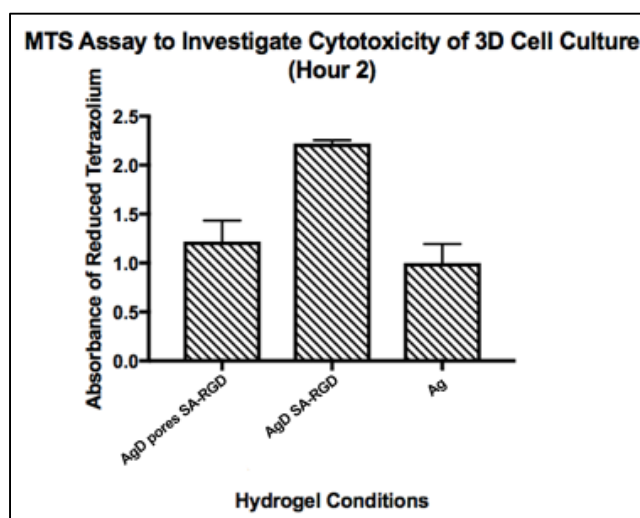
Figure 17: AgD gels with SA-RGD were determined to be non-cytotoxic when compared to bio-inert agarose gels by the MTS cell viability assay.

4. Discussion

We have developed a biomolecule immobilization system for hydrogels towards the development of 3D *in vitro* cell culture systems with exchangeable chemical properties. Peptide immobilization was achieved through the desthiobiotin-SA interaction since it forms a complex that is easily disrupted by biotin. Importantly, immobilization and displacement was not influenced by serum concentration (**Fig. S6**), indicating that the method is amenable to numerous cell culture conditions. The discovery and design of novel binding partners is increasing rapidly due to advances in computational design, *in vitro* selection and directed evolution. Therefore, this system could be redesigned with similar dynamic properties using different binding partners, or a combination of orthogonal binding partners to independently control the temporal patterning of different biomolecules. Different interactions other than desthiobiotin and SA may be investigated if the biological study will be influenced by desthiobiotin, biotin or SA.

Non-displaceable SA content is most likely due to positive charges present in AgD hydrogels. Biotin resulted in the displacement of ~90% of SA conjugates from hydrogels (**Fig. 5**); the remaining ~10% is non-displaceable and most likely due to non-specific binding (NSB). AgD contains primary amines (pKa ~ 10) that would be protonated at physiological pH and be at least partially responsible for the NSB of SA, which has a reported isoelectric point of 5.0.[96] Future experiments should quench the remaining amines to further minimize NSB.

Ideally, the temporal patterning system can be incorporated into any non-degradable bio-inert hydrogel with minimal NSB such as Ag, PEG or dextran. The

desthiobiotin content must remain constant over time for reproducible immobilization of biomolecules; the scaffold must therefore be non-degradable. Ag provides a bio-inert scaffold whose bioactivity can be readily tailored with immobilized biomolecules, which is crucial for our temporal patterning method. Although cells are able to penetrate Ag hydrogels, the small pore structure limits efficient cell penetration and migration.[24] Increased pores sizes may also improve washing affinity. Larger pores can be incorporated by introducing degradable porogens during hydrogel fabrication. Therefore, the temporal patterning system is currently being incorporated within hydrogels with larger pores to aid in cell seeding for future biological studies.

The desthiobiotin-SA immobilization method is amenable to any biomolecule that can be synthesized or expressed as a SA conjugate. In this study, we covalently linked a CGRGDS peptide to maleimide-SA; this approach is applicable to any peptide sequence containing cysteine. The bioactivity of SA-RGD was confirmed through cell adhesion studies (**Fig. 14**). Full proteins could also be immobilized by expressing them as a fusion protein with SA[97] or covalently conjugating a protein to SA using click chemistry. For example, maleimide-SA and a furan modified protein can be reacted together to form a SA-protein conjugate.[98]

The concentration of immobilized factors is an important regulator of bioactivity. For example, RGD-driven neurite outgrowth from dorsal root ganglions in 3D matrices is biphasic, where RGD concentrations outside the intermediate range limit outgrowth.[99] RGD concentration also influences the adhesion, proliferation and migration of mesenchymal stem cells encapsulated within hydrogels.[100] For the system described

here, the concentration of immobilized peptide can be varied by varying the amount of SA conjugates added during immobilization. For instance, the addition of 50 μL of 0.01 or 0.1 mg/ml SA solutions resulted in 0.23 and 2.2 μM immobilized SA. The immobilization of SA conjugates results in a gradient within the hydrogel, with the highest concentration at the surface. To explore this further, we quantified the vertical fluorescence profile of immobilized SA (**Fig. S5**). Fluorescence deviated by less than ~5% over the first 100 μm, which is similar to the maximum distance between cells and capillaries *in vivo*.[101] Large cell-hydrogel constructs are troublesome since they limit efficient supply of oxygen and nutrients and removal of waste products leading to necrosis and cell death. Therefore, our system is amenable to controlling the biochemical environment of hydrogels with similar diffusion distances for nutrients and waste products to those found *in vivo*.

The removal of reagents (e.g., SA conjugates and biotin) from the gel by diffusion is the rate limiting step for exchanging chemical environments. Minimizing washing times by decreasing hydrogel volume and increasing contact area with media will increase the efficiency of the system. The present study utilized 60 μL hydrogels in 96-well plates (**Figs. 5-6**), where only the surface of the gel is exposed to the media. To decrease washing times, we conjugated 20 μL hydrogels to glass surfaces using an amine-reactive silane (**Fig. 7**). Since the hydrogels contain 3.0 ± 0.5 μmol of amines per mmol of Ag, no further gel derivatization was required. These gels allow for more efficient washing due to their decreased size and greater surface exposure to the media. The efficiency of SA and biotin removal was increased by ~75% when hydrogel volumes were decreased from 60 to 20 μL (**Figs. 5-6, 9**).

AgD hydrogels with pores sizes ranging from 10 to 20 μm facilitated more efficient biochemical exchange and cell seeding, as porous hydrogels increase diffusion rates. Larger pore sizes decreased the time required for biochemical exchange from 48 h to 4.67 h hours in 60 μL gels (**Fig. 13**). Agarose gels prepared without porogens were not amenable to cell infiltration, whereas AgD gels with 10-20 μm pores was permissive for cell infiltration throughout the entire gel.

HUVEC tube formation was influenced by temporally altering hydrogel adhesivity, which is an important regulator of tube formation.[102] HUVECs were seeded on SA-RGD modified hydrogels. Once cell adhesion was confirmed (**Fig. 14A-C**), biotin was added to some SA-RGD AgD gels. Minimal differences between SA-RGD and SA-RGD with biotin conditions were observed after 6h of culture (2h of biotin exposure, **Fig. 14E-F**). After 24h of culture (20h of biotin exposure), HUVECs formed larger tube networks on SA-RGD gels than gels with SA-RGD and biotin, indicating decreased adhesion lowered tube formation potential (**Fig. 14H-I**). After 30h of culture (20h of biotin exposure), total tube length per gel for SA-RGD modified gels was significantly greater than gels with SA-RGD and biotin (**Fig. 14K-O**). These results indicate that HUVEC tube formation can be temporally controlled by exchanging hydrogel biochemical environments during *in vitro* cell culture experiments.

5. Conclusion

We have developed a temporal patterning system where we can immobilize desired biomolecules for multiple rounds by taking advantage of the physical interaction between desthiobiotin-streptavidin, which can be disrupted by biotin. We have reduced washing times by conjugating gels to the surface of glass slides, which decrease gel volume and increased relative gel-media contact area. We have also used alginate microparticles as sacrificial porogens to introduce pore sizes appropriate for cell seeding for 3D cell culture in AgD hydrogels. Overall, this porous, temporal patterning system in a scaffold appropriate for 3D cell culture will allow us to study cell-matrix interactions. We demonstrated the gels are non-cytotoxic and changes in biochemical environments can influence HUVEC tube formation. We also demonstrated cell viability in porous agarose hydrogels using an MTS assay.

6. References

1. Pampaloni F, Reynaud EG, Stelzer EHK. The third dimension bridges the gap between cell culture and live tissue. *Nat Rev Mol Cell Biol*. 2007;8(10):839-845. doi:10.1038/nrm2236.

2. Barrila, J., Radtke, A. L., Crabbé, A., Sarker, S. F., Herbst-Kralovetz, M. M., Ott, C. M., & Nickerson, C. A. (2010). Organotypic 3D cell culture models: using the rotating wall vessel to study host–pathogen interactions. *Nature Reviews Microbiology*, *8*(11), 791-801.

3. Hubbell, J. A. (1995). Biomaterials in tissue engineering. *Nature Biotechnology*, *13*(6), 565-576.

4. Antoni D, Burckel H, Josset E, Noel G. Three-Dimensional Cell Culture : A Breakthrough in Vivo. 2015:5517-5527. doi:10.3390/ijms16035517.

5. Baharvand H, Hashemi SM, Ashtiani SK, Farrokhi ALI. Differentiation of human embryonic stem cells into hepatocytes in 2D and 3D culture systems in vitro. 2006;652(January):645-652. doi:10.1387/ijdb.052072hb.

6. Mcbeath R, Pirone DM, Nelson CM, Bhadriraju K, Chen CS. Cell Shape , Cytoskeletal Tension , and RhoA Regulate Stem Cell Lineage Commitment. 2004;6:483-495.

7. Barralet JE, Wang L, Lawson M, Triffitt JT, Cooper PR. Comparison of bone marrow cell growth on 2D and 3D alginate hydrogels. 2005;6:515-519.

8. Tibbit, M. W., & Anseth, K. S. (2010). NIH Public Access, *103*(4), 655–663. http://doi.org/10.1002/bit.22361.Hydrogels as extracellular matrix mimics for 3D cell culture

9. Fischbach C, Chen R, Matsumoto T, et al. Engineering tumors with 3D scaffolds. 2007;4(10):6-11. doi:10.1038/NMETH1085.

10. Hynes RO. The Extracellular Matrix : Not Just Pretty Fibrils. 2009;326(November):1216-1220.

11. Frantz C, Stewart KM, Weaver VM, Frantz C, Stewart KM, Weaver VM. The extracellular matrix at a glance The Extracellular Matrix at a Glance. 2010;2010:4195-4200. doi:10.1242/jcs.023820.

12. Kadler KE, Baldock C, Bella J, Raymond P. Collagens at a glance. 2007;2007. doi:10.1242/jcs.03453.

13. Pankov R, Kenneth M. Fibronectin at a glance. 2002:3861-3863. doi:10.1242/jcs.00059.

14. Kresse, H., & Schönherr, E. (2001). Proteoglycans of the extracellular matrix and growth control. *Journal of cellular physiology*, *189*(3), 266-274.

15. Barrientos, S., Stojadinovic, O., Golinko, M. S., Brem, H., & Tomic-Canic, M. (2008). Growth factors and cytokines in wound healing. *Wound Repair and Regeneration*, *16*(5), 585-601.

16. Wight TN, Potter-perigo S. The extracellular matrix : an active or passive player in fibrosis ? 2011;98101(40):950-955. doi:10.1152/ajpgi.00132.2011

17. Schultz, G. S., & Wysocki, A. (2009). Interactions between extracellular matrix and growth factors in wound healing. *Wound repair and regeneration*, *17*(2), 153-162.

18. Brizzi, M. F., Tarone, G., & Defilippi, P. (2012). Extracellular matrix, integrins, and growth factors as tailors of the stem cell niche. *Current opinion in cell biology*, *24*(5), 645-651.

19. Azimifar, S. B., Böttcher, R. T., Zanivan, S., Grashoff, C., Krüger, M., Legate, K. R., ... & Fässler, R. (2012). Induction of membrane circular dorsal ruffles requires co-signalling of integrin–ILK-complex and EGF receptor. *J Cell Sci*, *125*(2), 435-448.

20. Deforest CA, Tirrell DA. Guiding stem cell fate in three-dimensional gels. 2015;14(February). doi:10.1038/NMAT4219.

21. Fuchs, E., Tumbar, T., & Guasch, G. (2004). Socializing with the neighbors: stem cells and their niche. *Cell*, *116*(6), 769-778.

22. Gattazzo, F., Urciuolo, A., & Bonaldo, P. (2014). Extracellular matrix: a dynamic microenvironment for stem cell niche. *Biochimica et Biophysica Acta (BBA)-General Subjects*, *1840*(8), 2506-2519.

23. Pickup, M. W., Mouw, J. K., & Weaver, V. M. (2014). The extracellular matrix modulates the hallmarks of cancer. *EMBO reports*, *15*(12), 1243-1253.

24. Balgude, A. P., Yu, X., Szymanski, A., & Bellamkonda, R. V. (2001). Agarose gel stiffness determines rate of DRG neurite extension in 3D cultures. *Biomaterials*, *22*(10), 1077-1084.

25. Augst, A. D., Kong, H. J., & Mooney, D. J. (2006). Alginate hydrogels as biomaterials. *Macromolecular bioscience*, *6*(8), 623-633.

26. Rowley, J. A., Madlambayan, G., & Mooney, D. J. (1999). Alginate hydrogels as synthetic extracellular matrix materials. *Biomaterials*, *20*(1), 45-53.

27. Chevallay, B., & Herbage, D. (2000). Collagen-based biomaterials as 3D scaffold for cell cultures: applications for tissue engineering and gene therapy. *Medical and Biological Engineering and Computing*, *38*(2), 211-218.

28. Burdick, J. A., & Prestwich, G. D. (2011). Hyaluronic acid hydrogels for biomedical applications. *Advanced materials*, *23*(12).

29. Na, K., won Kim, S., Sun, B. K., Woo, D. G., Yang, H. N., Chung, H. M., & Park, K. H. (2007). Osteogenic differentiation of rabbit mesenchymal stem cells in thermo-reversible hydrogel constructs containing hydroxyapatite and bone morphogenic protein-2 (BMP-2). *Biomaterials*, *28*(16), 2631-2637.

30. Kandow, C. E., Georges, P. C., Janmey, P. A., & Beningo, K. A. (2007). Polyacrylamide hydrogels for cell mechanics: steps toward optimization and alternative uses. *Methods in cell biology*, *83*, 29-46.

31. Lin, C. C., & Anseth, K. S. (2009). PEG hydrogels for the controlled release of biomolecules in regenerative medicine. *Pharmaceutical research*, *26*(3), 631-643.

32. Zhang, Z., Chen, S., & Jiang, S. (2006). Dual-functional biomimetic materials: nonfouling poly (carboxybetaine) with active functional groups for protein immobilization. *Biomacromolecules*, *7*(12), 3311-3315.

33. Smeets, N. M., Bakaic, E., Patenaude, M., & Hoare, T. (2014). Injectable and tunable poly (ethylene glycol) analogue hydrogels based on poly (oligoethylene glycol methacrylate). *Chemical Communications*, *50*(25), 3306-3309.

34. Kharkar, P. M., Kiick, K. L., & Kloxin, A. M. (2013). Designing degradable hydrogels for orthogonal control of cell microenvironments. *Chemical Society Reviews*, *42*(17), 7335-7372.

35. Anderson, S. B., Lin, C. C., Kuntzler, D. V., & Anseth, K. S. (2011). The performance of human mesenchymal stem cells encapsulated in cell-degradable polymer-peptide hydrogels. *Biomaterials*, *32*(14), 3564-3574.

36. Ashton, R. S., Banerjee, A., Punyani, S., Schaffer, D. V., & Kane, R. S. (2007). Scaffolds based on degradable alginate hydrogels and poly (lactide-co-glycolide) microspheres for stem cell culture. *Biomaterials*, *28*(36), 5518-5525.

37. Jeon, O., Bouhadir, K. H., Mansour, J. M., & Alsberg, E. (2009). Photocrosslinked alginate hydrogels with tunable biodegradation rates and mechanical properties. *Biomaterials*, *30*(14), 2724-2734.

38. Chiu, Y. C., Cheng, M. H., Engel, H., Kao, S. W., Larson, J. C., Gupta, S., & Brey, E. M. (2011). The role of pore size on vascularization and tissue remodeling in PEG hydrogels. *Biomaterials*, *32*(26), 6045-6051.

39. Zeltinger, J., Sherwood, J. K., Graham, D. A., Müeller, R., & Griffith, L. G. (2001). Effect of pore size and void fraction on cellular adhesion, proliferation, and matrix deposition. *Tissue engineering*, *7*(5), 557-572.

40. Huebsch, N., Lippens, E., Lee, K., Mehta, M., Koshy, S. T., Darnell, M. C., ... & Chaudhuri, O. (2015). Matrix elasticity of void-forming hydrogels controls transplanted-stem-cell-mediated bone formation. *Nature materials*, *14*(12), 1269-1277.

41. Eiselt, P., Yeh, J., Latvala, R. K., Shea, L. D., & Mooney, D. J. (2000). Porous carriers for biomedical applications based on alginate hydrogels. *Biomaterials*, *21*(19), 1921-1927.

42. Chen, J., Park, H., & Park, K. (1999). Synthesis of superporous hydrogels: hydrogels with fast swelling and superabsorbent properties. *Journal of Biomedical Materials Research Part A*, *44*(1), 53-62.

43. Lee, K. Y., Rowley, J. A., Eiselt, P., Moy, E. M., Bouhadir, K. H., & Mooney, D. J. (2000). Controlling mechanical and swelling properties of alginate hydrogels independently by cross-linker type and cross-linking density. *Macromolecules*, *33*(11), 4291-4294.

44. Saraydın, D., Karadag, E., Işıkver, Y., Şahiner, N., & Güven, O. (2004). The influence of preparation methods on the swelling and network properties of acrylamide hydrogels with crosslinkers. *Journal of Macromolecular Science, Part A*, *41*(4), 419-431.

45. Kloxin, April M., Mark W. Tibbitt, Andrea M. Kasko, Jonathan A. Fairbairn, and Kristi S. Anseth. "Tunable hydrogels for external manipulation of cellular microenvironments through controlled photodegradation." *Advanced Materials* 22, no. 1 (2010): 61-66.

46. Kim, T. K., Yoon, J. J., Lee, D. S., & Park, T. G. (2006). Gas foamed open porous biodegradable polymeric microspheres. *Biomaterials*, *27*(2), 152-159.

47. Reis, C. P., Ribeiro, A. J., Neufeld, R. J., & Veiga, F. (2007). Alginate microparticles as novel carrier for oral insulin delivery. *Biotechnology and bioengineering*, *96*(5), 977-989.

48. Lee, K. Y., & Mooney, D. J. (2012). Alginate: properties and biomedical applications. *Progress in polymer science*, *37*(1), 106-126.

49. Omidian, H., Rocca, J. G., & Park, K. (2005). Advances in superporous hydrogels. *Journal of Controlled Release*, *102*(1), 3-12.

50. Kabiri, K., H. Omidian, and M. J. Zohuriaan-Mehr. "Novel approach to highly porous superabsorbent hydrogels: synergistic effect of porogens on porosity and swelling rate." *Polymer International* 52.7 (2003): 1158-1164.

51. Kim, D., & Park, K. (2004). Swelling and mechanical properties of superporous hydrogels of poly (acrylamide-co-acrylic acid)/polyethylenimine interpenetrating polymer networks. *Polymer*, *45*(1), 189-196.

52. Lee, K. Y., Rowley, J. A., Eiselt, P., Moy, E. M., Bouhadir, K. H., & Mooney, D. J. (2000). Controlling mechanical and swelling properties of alginate hydrogels independently by cross-linker type and cross-linking density. *Macromolecules*, *33*(11), 4291-4294.

53. Jeon, O., Bouhadir, K. H., Mansour, J. M., & Alsberg, E. (2009). Photocrosslinked alginate hydrogels with tunable biodegradation rates and mechanical properties. *Biomaterials*, *30*(14), 2724-2734.

54. Hodgson, S. M. (2017). *Poly (ethylene glycol) Hydrogels Crosslinked via the Strain-Promoted Alkyne-Azide Cycloaddition* (Doctoral dissertation).

55. Bouhadir, K. H., Hausman, D. S., & Mooney, D. J. (1999). Synthesis of cross-linked poly (aldehyde guluronate) hydrogels. *Polymer*, *40*(12), 3575-3584.

56. Phelps, E. A., Enemchukwu, N. O., Fiore, V. F., Sy, J. C., Murthy, N., Sulchek, T. A., ... & García, A. J. (2012). Maleimide cross-linked bioactive peg hydrogel exhibits improved reaction kinetics and cross-linking for cell encapsulation and in situ delivery. *Advanced materials*, *24*(1), 64-70.

57. Nimmo, C. M., Owen, S. C., & Shoichet, M. S. (2011). Diels– Alder click cross-linked hyaluronic acid hydrogels for tissue engineering. *Biomacromolecules*, *12*(3), 824-830.

58. Wei, H. L., Yang, Z., Zheng, L. M., & Shen, Y. M. (2009). Thermosensitive hydrogels synthesized by fast Diels–Alder reaction in water. *Polymer*, *50*(13), 2836-2840.

59. Vetrík, M., Přádný, M., Hrubý, M., & Michálek, J. (2011). Hydrazone-based hydrogel hydrolytically degradable in acidic environment. *Polymer degradation and stability*, *96*(5), 756-759.

60. Kuo, C. K., & Ma, P. X. (2001). Ionically crosslinked alginate hydrogels as scaffolds for tissue engineering: part 1. Structure, gelation rate and mechanical properties. *Biomaterials*, *22*(6), 511-521.

61. Nakahata, M., Takashima, Y., Yamaguchi, H., & Harada, A. (2011). Redox-responsive self-healing materials formed from host–guest polymers. *Nature communications*, *2*, 511.

62. Sarkar, N. (1979). Thermal gelation properties of methyl and hydroxypropyl methylcellulose. *Journal of applied polymer science*, *24*(4), 1073-1087.

63. Nguyen, K. T., & West, J. L. (2002). Photopolymerizable hydrogels for tissue engineering applications. *Biomaterials*, *23*(22), 4307-4314.

64. Lecamp, L., Houllier, F., Youssef, B., & Bunel, C. (2001). Photoinitiated cross-linking of a thiol–methacrylate system. *Polymer*, *42*(7), 2727-2736.

65. Hahn, M. S., Miller, J. S., & West, J. L. (2006). Three-dimensional biochemical and biomechanical patterning of hydrogels for guiding cell behavior. *Advanced Materials*, *18*(20), 2679-2684.

66. Nuttelman, C. R., Mortisen, D. J., Henry, S. M., & Anseth, K. S. (2001). Attachment of fibronectin to poly (vinyl alcohol) hydrogels promotes NIH3T3 cell adhesion, proliferation, and migration. *Journal of Biomedical Materials Research Part A*, *57*(2), 217-223.

67. Barbucci, R., Rappuoli, R., Borzacchiello, A., & Ambrosio, L. (2000). Synthesis, chemical and rheological characterization of new hyaluronic acid-based hydrogels. *Journal of Biomaterials Science, Polymer Edition*, *11*(4), 383-399.

68. Nair, D. P., Podgórski, M., Chatani, S., Gong, T., Xi, W., Fenoli, C. R., & Bowman, C. N. (2013). The thiol-Michael addition click reaction: a powerful and widely used tool in materials chemistry. *Chemistry of Materials*, *26*(1), 724-744.

69. Lutolf, M. P., Raeber, G. P., Zisch, A. H., Tirelli, N., & Hubbell, J. A. (2003). Cell-Responsive Synthetic Hydrogels. *Advanced Materials*, *15*(11), 888-892.

70. Mather, B. D., Viswanathan, K., Miller, K. M., & Long, T. E. (2006). Michael addition reactions in macromolecular design for emerging technologies. *Progress in Polymer Science*, *31*(5), 487-531.

71. Yeo, W. S., Yousaf, M. N., & Mrksich, M. (2003). Dynamic interfaces between cells and surfaces: electroactive substrates that sequentially release and attach cells. *Journal of the American Chemical Society*, *125*(49), 14994-14995.

72. Evans, R. A. (2007). The rise of azide–alkyne 1, 3-dipolar 'click'cycloaddition and its application to polymer science and surface modification. *Australian Journal of Chemistry*, *60*(6), 384-395.

73. Yu, F., Cao, X., Li, Y., Zeng, L., Yuan, B., & Chen, X. (2014). An injectable hyaluronic acid/PEG hydrogel for cartilage tissue engineering formed by integrating enzymatic crosslinking and Diels–Alder "click chemistry". *Polymer Chemistry*, *5*(3), 1082-1090.

74. Lutz, J. F., & Zarafshani, Z. (2008). Efficient construction of therapeutics, bioconjugates, biomaterials and bioactive surfaces using azide–alkyne "click" chemistry. *Advanced drug delivery reviews*, *60*(9), 958-970.

75. Yu, H., Li, J., Wu, D., Qiu, Z., & Zhang, Y. (2010). Chemistry and biological applications of photo-labile organic molecules. *Chemical Society Reviews*, *39*(2), 464-473.

76. Shigeri, Y., Tatsu, Y., & Yumoto, N. (2001). Synthesis and application of caged peptides and proteins. *Pharmacology & therapeutics*, *91*(2), 85-92.

77. Yang, W., & Rånby, B. (1996). Radical living graft polymerization on the surface of polymeric materials. *Macromolecules*, *29*(9), 3308-3310.

78. Goubko, C. A., Majumdar, S., Basak, A., & Cao, X. (2010). Hydrogel cell patterning incorporating photocaged RGDS peptides. *Biomedical microdevices*, *12*(3), 555-568.

79. Goubko, C. A., Basak, A., Majumdar, S., & Cao, X. (2014). Dynamic cell patterning of photoresponsive hyaluronic acid hydrogels. *Journal of Biomedical Materials Research Part A*, *102*(2), 381-391.

80. Polizzotti, B. D., Fairbanks, B. D., & Anseth, K. S. (2008). Three-dimensional biochemical patterning of click-based composite hydrogels via thiolene photopolymerization. *Biomacromolecules*, *9*(4), 1084-1087.

81. Weber, P. C., Ohlendorf, D. H., Wendoloski, J. J., & Salemme, F. R. (1989). Structural origins of high-affinity biotin binding to streptavidin. *Science*, *243*(4887), 85-88.

82. Hartley, R. W. (1989). Barnase and barstar: two small proteins to fold and fit together. *Trends in biochemical sciences*, *14*(11), 450-454.

83. Li, Y., & Sousa, R. (2012). Expression and purification of E. coli BirA biotin ligase for in vitro biotinylation. *Protein expression and purification*, *82*(1), 162-167.

84. Segura, T., Anderson, B. C., Chung, P. H., Webber, R. E., Shull, K. R., & Shea, L. D. (2005). Crosslinked hyaluronic acid hydrogels: a strategy to functionalize and pattern. *Biomaterials*, *26*(4), 359-371.

85. Wylie, R. G., Ahsan, S., Aizawa, Y., Maxwell, K. L., Morshead, C. M., & Shoichet, M. S. (2011). Spatially controlled simultaneous patterning of multiple growth factors in three-dimensional hydrogels. *Nature materials*, *10*(10), 799-806.

86. Tibbitt, M. W., & Anseth, K. S. (2009). Hydrogels as extracellular matrix mimics for 3D cell culture. *Biotechnology and bioengineering*, *103*(4), 655-663.

87. DeForest, C. A., & Anseth, K. S. (2012). Photoreversible Patterning of Biomolecules within Click-Based Hydrogels. *Angewandte Chemie*, *124*(8), 1852-1855.

88. DeForest, C. A., & Tirrell, D. A. (2015). A photoreversible protein-patterning approach for guiding stem cell fate in three-dimensional gels. *Nature materials*, *14*(5), 523-531.

89. Boekhoven, J., Rubert Pérez, C. M., Sur, S., Worthy, A., & Stupp, S. I. (2013). Dynamic display of bioactivity through host–guest chemistry. *Angewandte Chemie International Edition*, *52*(46), 12077-12080.

90. Pan, G., Guo, B., Ma, Y., Cui, W., He, F., Li, B., ... & Shea, K. J. (2014). Dynamic introduction of cell adhesive factor via reversible multicovalent phenylboronic acid/cis-diol polymeric complexes. *Journal of the American Chemical Society*, *136*(17), 6203-6206.

91. Morgan, H., & Taylor, D. M. (1992). A surface plasmon resonance immunosensor based on the streptavidin-biotin complex. *Biosensors and Bioelectronics*, *7*(6), 405-410.

92. Mann, B. K., Tsai, A. T., Scott-Burden, T., & West, J. L. (1999). Modification of surfaces with cell adhesion peptides alters extracellular matrix deposition. *Biomaterials*, *20*(23), 2281-2286.

93. Gunawan, R. C., King, J. A., Lee, B. P., Messersmith, P. B., & Miller, W. M. (2007). Surface presentation of bioactive ligands in a nonadhesive background using DOPA-tethered biotinylated poly (ethylene glycol). *Langmuir*, *23*(21), 10635-10643.

94. Hirsch, J. D., Eslamizar, L., Filanoski, B. J., Malekzadeh, N., Haugland, R. P., Beechem, J. M., & Haugland, R. P. (2002). Easily reversible desthiobiotin binding to streptavidin, avidin, and other biotin-binding proteins: uses for protein labeling, detection, and isolation. *Analytical biochemistry*, *308*(2), 343-357.

95. Pernodet, N., Maaloum, M., & Tinland, B. (1997). Pore size of agarose gels by atomic force microscopy. *Electrophoresis*, *18*(1), 55-58.

96. Sivasankar, S., Subramaniam, S., & Leckband, D. (1998). Direct molecular level measurements of the electrostatic properties of a protein surface. *Proceedings of the National Academy of Sciences*, *95*(22), 12961-12966.

97. Schultz, J., Lin, Y., Sanderson, J., Zuo, Y., Stone, D., Mallett, R., ... & Axworthy, D. (2000). A tetravalent single-chain antibody-streptavidin fusion protein for pretargeted lymphoma therapy. *Cancer research*, *60*(23), 6663-6669.

98. Heredia, K. L., & Maynard, H. D. (2006). Synthesis of protein–polymer conjugates. *Organic & Biomolecular Chemistry*, *5*(1), 45-53.

99. Schense, J. C., & Hubbell, J. A. (2000). Three-dimensional migration of neurites is mediated by adhesion site density and affinity. *Journal of Biological Chemistry*, *275*(10), 6813-6818.

100. Salinas, C. N., & Anseth, K. S. (2008). The enhancement of chondrogenic differentiation of human mesenchymal stem cells by enzymatically regulated RGD functionalities. *Biomaterials*, *29*(15), 2370-2377.

101. Lovett, M., Lee, K., Edwards, A., & Kaplan, D. L. (2009). Vascularization strategies for tissue engineering. *Tissue Engineering Part B: Reviews*, *15*(3), 353-370.

102. Saunders, R. L., & Hammer, D. A. (2010). Assembly of human umbilical vein endothelial cells on compliant hydrogels. *Cellular and molecular bioengineering*, *3*(1), 60-67.

7. Appendix

Appendix A: Materials and Methods

Materials

Agarose type IX, bovine serum albumin, desthiobiotin, carbonyl diimidazole (CDI), trimethylamine, 1-Ethyl-3-(3-dimethylaminopropyl)carbodiimide (EDC), N-hydroxysuccinimide (NHS), N-(2-aminoethyl)acetamide, fluorescamine and maleimide-streptavidin were purchased from Sigma-Aldrich (Oakville, ON). Biotin was purchased from Bioshop Canada Inc. (Burlington, ON). Alexa Fluor® 488 NHS ester, streptavidin-Alexa Fluor® 488 (SA-488), streptavidin-Alexa Fluor® 647 (SA-647) conjugates, and Calcein AM were purchased from Thermo Fisher Scientific (Burlington, ON). CGRGDS peptide was purchased from Genscript (Piscataway, NJ). Human umbilical vein endothelial cells (HUVECs), NIH 3T3 fibroblasts, endothelial cell growth medium (EGM™-2), and calf bovine serum (CBS) were purchased from Cedarlane (Burlington, ON). Dialysis tubing (MWCO 3,500 and 10,000 Da) was purchased from Spectrum Labs (Rancho Dominguez, CA). PRONOVA™ ultrapure sodium alginate was purchased from NovaMatrix (Sandvika, Norway).

Synthesis of Agarose Desthiobiotin

500 mg of agarose, 46 mg of CDI and 236 μL of triethylamine were dissolved in 50 mL of DMSO and stirred at room temperature under nitrogen. After 1h, 57 μL of ethylene diamine was added. After 16h, the agarose solution was diluted to 1 mg/mL with warm water and dialyzed (MWCO 3,500 da) against distilled water with 6 water

exchanges. The polymer agarose-amine solution was lyophilized to yield 490 mg. 120 mg of desthiobiotin was reacted with 325 mg of EDC and 200 mg of NHS in 20 mL of chloroform under nitrogen. After one day, chloroform was removed under vacuum, solid was re-dissolved in 20 mL of DMSO and added to 490 mg of agarose-amine and 100 μL of trimethylamine (TEA) in 50 mL of DMSO. After stirring under nitrogen for one day, the solution was diluted with 250 mL of warm water and dialyzed (MWCO 3,500 Da) against distilled water with 6 water exchanges. Lyophilization yielded 410 mg of AgD.

Desthiobiotin Quantification

The Thermo Scientific Fluorescence Biotin Quantitation assay procedure was modified to quantify desthiobiotin derivatization of AgD polymers. The provided DyLight reporter solution was diluted 1:15 with pH 7.4 PBS, and 90 μL was mixed with 10 μL of 0.7 μg/mL agarose samples in PBS (n=3). After five minutes, fluorescence was measured (λ_{ex} = 494 nm; λ_{em} = 520 nm) using a plate reader. Desthiobiotin concentrations were calculated from a desthiobiotin calibration curve of 0.5 to 6 μM solutions in PBS.

Fluorescamine assays were performed by mixing 50 μL of agarose samples in DMSO with a 50 μL of 6 mM fluorescamine-DMSO solution with 10 mM TEA. After 30 minutes, fluorescence of the samples was measured (λ_{ex} = 395 nm; λ_{em} = 485 nm) using a plate reader (Tecan Sapphire). A calibration curve was constructed with N-(2-aminoethyl)acetamide solutions of 5 to 320 μM.

SA conjugate binding studies in AgD hydrogels (microplate binding study)

Solutions of 0.7 or 1 wt% AgD were prepared by dissolving the lyophilized solid in hot PBS (pH 7.4). 60 μL of AgD solutions was pipetted into 96 well plates, and cast at

4°C for 1h; plates were then immersed in PBS for 1 days to remove remaining unconjugated desthiobiotin molecules. 50 µL of fluorescent SA-488 in PBS with 0.5 mg/ml BSA was added over each gel. After overnight incubation, plates were immersed in PBS with 0.5 mg/mL BSA, and fluorescence was read (λ_{ex} = 490 nm; λ_{em} = 525 nm, gain 155 for SA-488; λ_{ex} = 594 nm; λ_{em} = 633 nm, gain 193 for SA-647). After excess SA-488 was removed, plates were immersed in the displacement solution (0.5 mg/mL BSA and biotin in PBS), and fluorescence was tracked over time. Plates were submerged in PBS with 0.5 mg/mL BSA to remove excess biotin. To repeat functionalization, the gels were then re-exposed to fluorescent SA, rinsed and exposed to biotin. To demonstrate temporal control of the chemical environment serum solutions, all steps were conducted in a biosafety cabinet under sterile conditions.

To demonstrate temporal control of chemical environment, variations of the experiment were performed where gels were exposed to: (1) 0.01 mg/mL SA-488 for all three repetitions; (2) 0.01 mg/mL SA-488, followed by 0.01 mg/mL SA-647, then 0.01 mg/mL of both SA-488 and SA-647; and, (3) 0.0075 mg/mL SA-488 with 0.0025 mg/mL SA-647, followed by 0.005 mg/mL of both SA conjugates, and 0.0025 mg/mL SA-488 with 0.0075 mg/mL SA-647.

To calculate protein concentrations, fluorescence of 60 µL agarose hydrogels containing known concentrations of fluorescent SAs was read.

Fluorescent Streptavidin Binding Experiments in 1% CBS

The conditions were: (1) 0.1 mg/mL SA-488 for two repetitions; (2) 0.1 mg/mL SA-488 followed by 0.1 mg/mL SA-647; (3) 0.075 mg/mL SA-488 with 0.025 mg/mL

SA-647, followed by 0.05 mg/mL of both SA conjugates, and 0.025 mg/mL SA-488 with 0.075 mg/mL SA-647; and, (4) 0.1 mg/mL SA-RGD-488, followed by 0.075 mg/mL SA-RGD-488 with 0.025 mg/mL SA-647, and 0.025 mg/mL SA-RGD-488 with 0.075 mg/mL SA-647. To maintain sterility, PBS was autoclaved prior to use, fluorescent SA solutions in PBS were filtered (0.2 μm), and experiments were performed in a biosafety cabinet.

Conjugation of 20 μL AgD hydrogels to glass slides

Glass slides were cleaned in a 3M KOH solution, washed with water, and dried overnight at 120ºC. 3 or 4 drops of a 1.5% hydroxyl(polyethyleneoxy)propyl triethoxysilane solution in dry methanol was applied and spin coated (5000 rpm for 30 seconds) on the surface of the glass slides. After drying at 95ºC for 4 h, the slides were placed in 15 mL of a 5 mg/mL solution of CDI in dichloromethane (DCM) for 24h. Slides were rinsed in DCM and dried at 95ºC for 4h. Hydrophobic circles with an inner diameter of 5 mm were created on the slides using a PAP pen. 20μL of a 1 wt% AgD solution in PBS were pipetted within the hydrophobic circles and gelled at 4ºC.

AgD binding study with 1 wt% hydrogels (glass slides)

40 μL of 0.01 mg/mL SA-488 in PBS was pipetted on top of the gels. Washing and biotin displacement steps were conducted in 200 mL of PBS with 0.5 mg/mL of BSA and PBS with 0.5 mg/mL of biotin and BSA, respectively. Hydrogel fluorescence was quantified using fluorescence microscopy, and analyzed in ImageJ using identical regions of interest in multiple hydrogels. AgD gels not exposed to SA-488 were used as controls. The corrected total fluorescence (CTF) was calculated using the following equation: CTF

= Integrated Density – (Selected area x Mean fluorescence of background readings). The average CTF of the hydrogels was then calculated (n=3, mean ± standard deviation).

Alginate microparticle fabrication and pore formation within AgD hydrogels

Alginate particles were first prepared by a previously published emulsion technique.[27] 8.3 mL of a 5% (w/v) aqueous dispersion of insoluble calcium carbonate crystals was sonicated for 30 minutes. After sonication, the aqueous 5% w/v calcium carbonate mixture was combined with 50 mL of a 2% sodium alginate solution, and mixed by impeller stirring at 500 RPM for 15 minutes. 58.3 mL of a paraffin oil containing 3% Span 80 was added to the mixture and emulsified by impeller stirring at 1600 RPM for 15 minutes. 20 mL of paraffin oil with 830 µL of glacial acetic acid was added, and the resultant mixture was mixed for 60 minutes at 1600 RPM. The particles were isolated by centrifugation at 15,000 x g for 15 minutes. Particles were washed 6 times with an acetone (15%), isopropanol (10%), hexane (5%), and acetate buffer (pH 4.5, 70%) mixture, followed by an overnight incubation in a 2% Tween 20/CaCl$_2$ solution. Particles were the washed in a 2% Tween 20/CaCl$_2$ solution an additional 6 times. Alginate particles were stored in a MES/CaCl$_2$ buffer solution at 4°C.

Falcon tubes containing alginate particles in a MES/CaCl$_2$ buffer were inverted to suspend alginate particles. 100 µL of the suspended alginate particles was transferred into each microcentrifuge tubes. The microcentrifuge tubes were then centrifuged to pellet the large alginate particles. The supernatant was discarded, and the large alginate particles were combined into one microcentrifuge tube using a scoopula. Simultaneously, a 1wt% AgD gel was melted and cooled, and then mixed with the alginate particles in a 2:1 AgD

to particle ratio. 60 µL of the mixture was dispensed into wells of a 96 well microplate. The cell culture plate was quickly placed at 4°C for rapid gelation. After gelation, 100 µL of 0.5M EDTA was added to each, and left overnight to degrade the alginate particles. the gels were then immersed in PBS to remove dissolved alginate and EDTA.

Characterizing pore size in AgD hydrogels

AgD gels were labelled with SA-488 and imaged on a Nikon confocal microscope. Cell culture plates were inverted and aligned with the 20X objective lens. First, the bright field function and ocular lens were used to identify the surface of the microplate, and the bottom of the hydrogel. Images of single slices, and z – stacks were acquired.

Seeding and imaging 3T3 mouse fibroblast cells within porous AgD Hydrogels

60 µL porous AgD hydrogels were incubated with 50 µL of 0.2 mg/mL SA-RGD. After an overnight incubation, the hydrogels were washed in 250 mL of PBS. Fibroblasts were then added to the gels in DMEM media with 10% CBS and incubated at 37°C 5% CO_2 for 24 hours. Cells were then stained with 1 µL of Calcein AM. Cells were imaged using a fluorescent microscope (BioTek Cytation5).

Evaluating cytotoxicity

The CellTiter 96® AQ$_{ueous}$ One Solution Cell Proliferation Assay (MTS) was used to evaluate cytotoxicity of the AgD cell culture system. 60 μL AgD hydrogels were pre-incubated overnight in DMEM media with 10% CBS. Fibroblasts (approximately 800,000-1,000,000 cells/mL) were added in DMEM media with 10% CBS and incubated at 37°C and 5% CO_2 overnight. 20 µL of CellTiter 96 AQueous One Solution Reagent

was pipetted into each well. After a 60-minute incubation, the absorbance at 490 nm was read.

Human umbilical vein endothelial cell (HUVEC) adhesion and tube formation assay.

10,000 HUVECs were seeded onto 60 µL 2 wt% AgD and SA-RGD modified AgD hydrogels in EGM-2 media. SA-RGD modified AgD hydrogels were prepared by incubating hydrogels in 200 µL of PBS with 0.05 mg/ml SA-RGD and 0.5 mg/mL BSA for 2 days. The gels were then washed for 2 days in PBS with BSA to remove excess SA-RGD. Brightfield images were acquired 3 h after cell seeding, and cell circularity was determined using Image J. 4h after cell seeding, the media for 3 AgD SA-RGD gels was exchanged to EGM-2 with 0.5 mg/ml of biotin. Media in all other samples was replenished to maintain consistency. After 6 and 24 h, brightfield images were acquired. After 30h, cells were stained with Calcein Am and fluorescent images were acquired. Total tube length per well was assessed in Image J for each condition. (n=3, mean ± standard deviation)
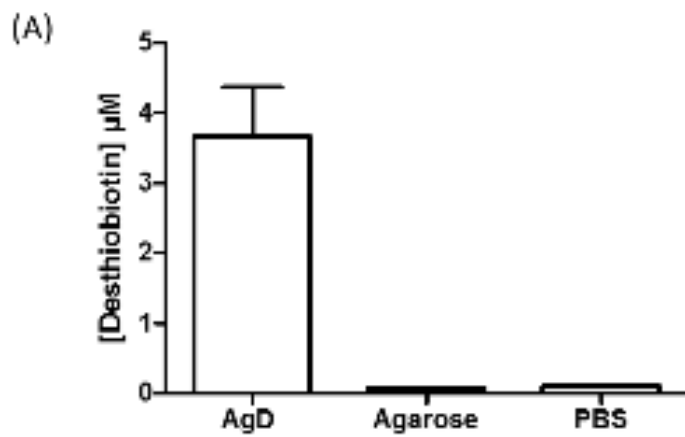
Appendix B: Supplemental figures

Figure S1: Desthiobiotin concentration was calculated through a fluorescent biotin quantification assay. AgD contained 1.7 ± 0.5 μmol desthiobiotin per mmol of Ag subunit.
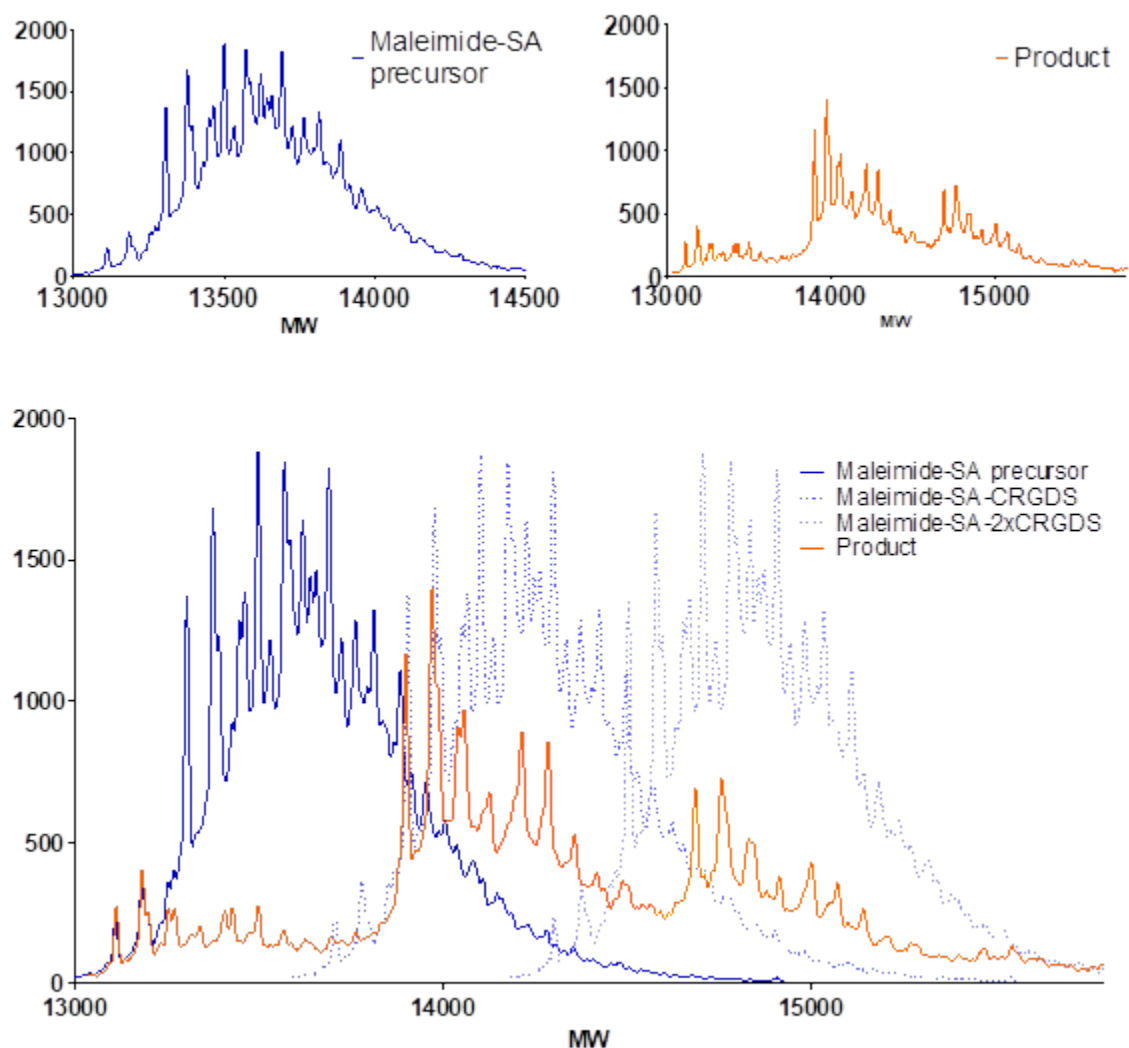
Figure S2: MALDI of SA-RGD. (A) MALDI of maleimide-SA showing the monomer. (B) MALDI of SA-RGD showing the monomer. (C) Combined MALDIs of (A) and (B) with theoretical projections of SA monomer with 1 or 2 CGRGDS peptides (dashed blue lines). The majority of SA monomers were labelled with 1 or 2 peptides, indicating tetrameric SA contains between 4 and 8 GRGDS peptides.
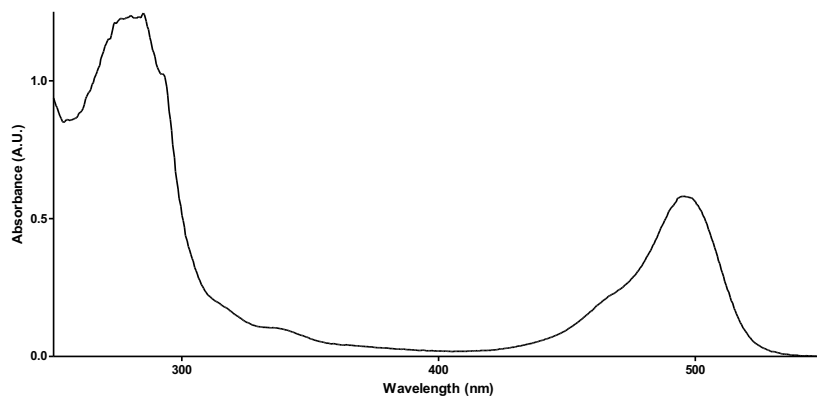
Figure S3: UV-Vis spectrum of SA-RGD-488 showing the protein peak at 280 nm and
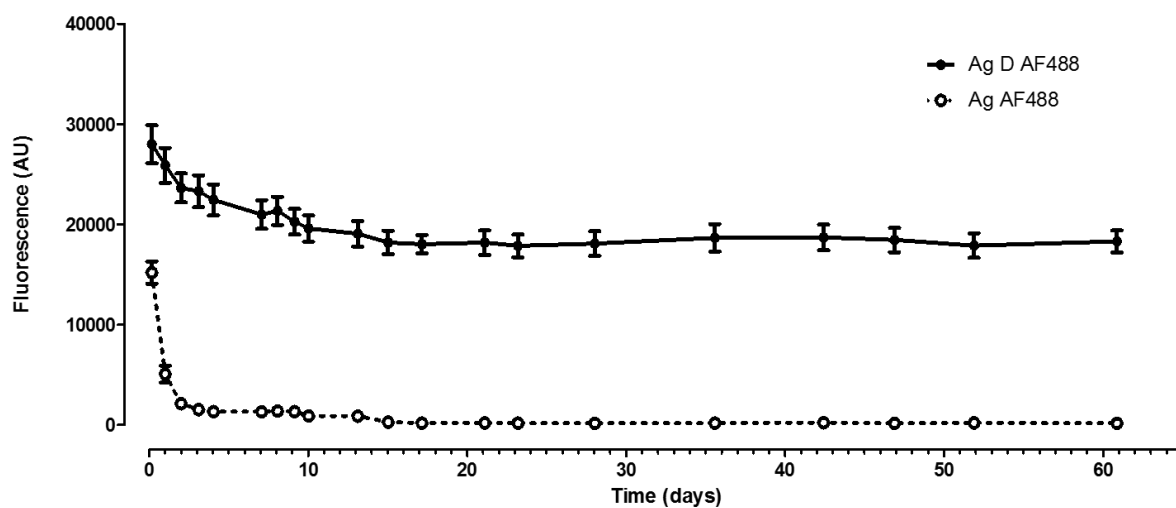
the Alexa 488 peak at 495 nm.

Figure S4: SA-488 immobilized in AgD hydrogels remains stable for over 60 days. AgD and Ag hydrogels were incubated in SA-488 solutions then washed in PBS. Fluorescence rapidly dropped in Ag hydrogels, but AgD fluorescence remained stable due to the desthiobiotin-streptavidin interaction (mean ± standard deviation; n=16).
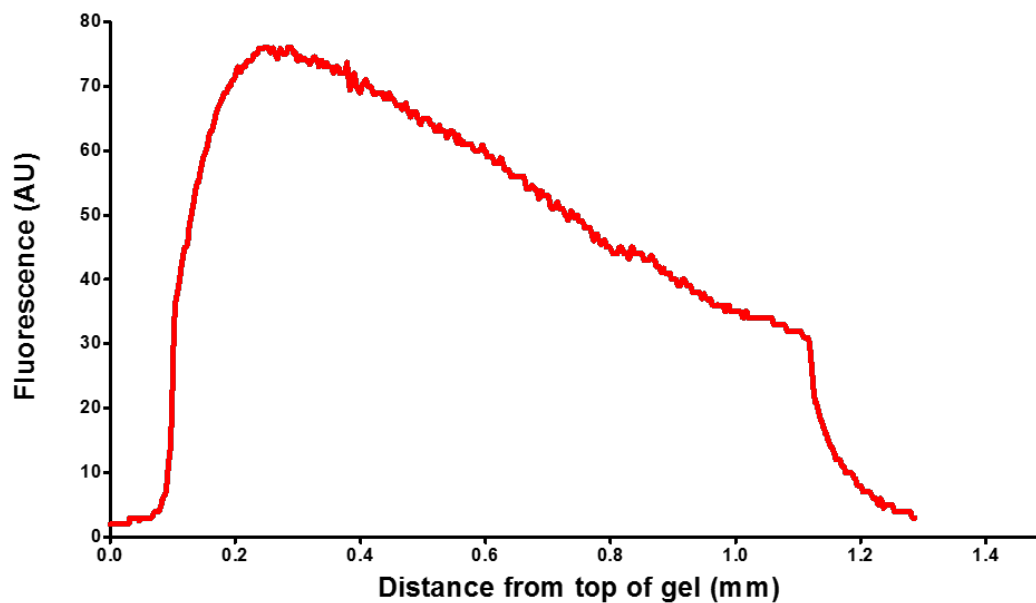
Figure S5: Vertical fluorescence profile of SA-488 immobilized in AgD hydrogels. The rapid rise in fluorescence between ~0 and 0.25 μm is due to the meniscus of the hydrogel. The remainder of the hydrogel (from ~0.25 to 1.1 μm) saw a decrease of ~59% in fluorescence as a function of depth. The first 200 μm, the relevant distance for cell-hydrogel constructs, only decreased ~9% in fluorescence.
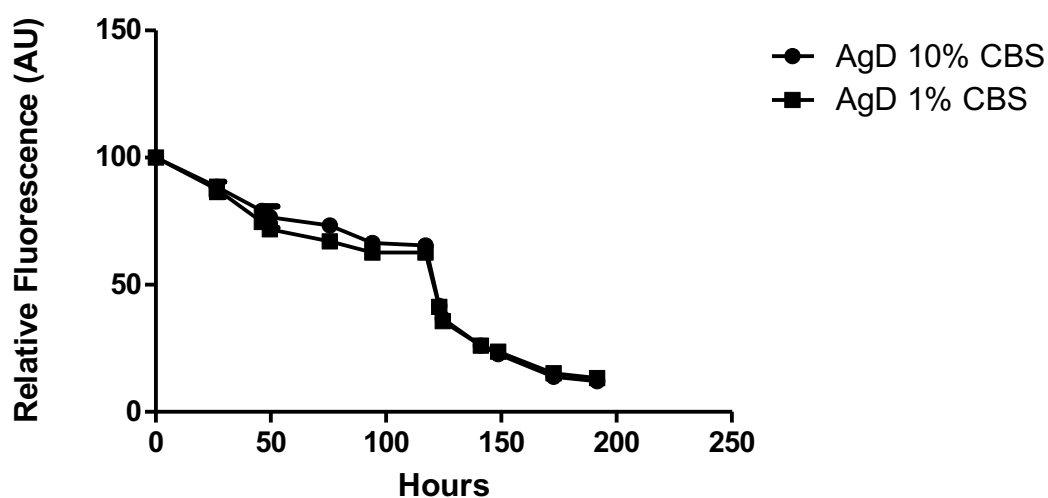
Figure S6: Immobilization and displacement of SA-488 in 0.7wt% AgD hydrogels exposed to 1 or 10% serum. Fluorescence intensities were normalized to 100 for t=0 h. 50 µL of 0.1 mg/ml SA-488 solutions were pipetted on the gels, and left for 17 h. Gels were then washed in ~400 mL of PBS with either 1 or 10% CBS. After 117h, 0.5 mg/ml biotin was added to the PBS/CBS solutions to displace immobilized SA-488 (mean ± standard deviation; n=3).